Ind. Eng. Chem. Res. **2001,** *40,* 319−337

Adsorption of C_1−C_7 Normal Alkanes on BAX-Activated Carbon. 2. Statistically Optimized Approach for Deriving Thermodynamic Properties from the Adsorption Isotherm

Shaheen A. Al-Muhtaseb, Charles E. Holland, and James A. Ritter*

Department of Chemical Engineering, Swearingen Engineering Center, University of South Carolina, Columbia, South Carolina 29208

A new stepwise (SW) statistically optimized model and also a virial-type (VT) model were correlated successfully with adsorption equilibria for the *n*-alkane series C_1−C_7 on Westvaco BAX-1100 activated carbon over a wide range of temperatures and pressures. Both models predicted reasonable temperature-dependent isosteric heats of adsorption, and from these slight dependencies, sensible deviations between the adsorbed- and gas-phase heat capacities were indicated. However, the SW model was more reliable under extreme conditions. The SW model also showed that the observed linear dependence of ln(P) on $1/T$ at constant loading, according to the Clausius−Clapeyron equation, only occasionally contributed to the overall description; statistically, more complicated temperature dependencies of ln(P) were revealed, indicating that the temperature dependence of the isosteric heat of adsorption can be easily overlooked. The ideal-gas assumption, inherent in the Clausius−Clapeyron equation, was also relaxed. The resulting real-gas isosteric heats of adsorption were reduced compared to the ideal-gas values, especially at high loadings and high temperatures. Finally, the temperature-independent isosteric heats of adsorption predicted from the potential theory correlation developed in Part 1 of this series fell almost in the exact middle of the range predicted by the temperature-dependent SW and VT models for the lightly to moderately adsorbed alkanes, but severely underpredicted those for the heavily adsorbed alkanes (i.e., heavier than *n*-propane).

Introduction

The reliable estimation of derived thermodynamic properties, such as the isosteric heat of adsorption and the adsorbed-phase heat capacity, is one of the most important cornerstones for the realistic design and simulation of different nonisothermal adsorption processes. Such properties also provide significant information about the physical character of specific adsorption systems, including adsorbent surface heterogeneity and adsorbate−adsorbate lateral interactions.[1,2] The most reliable estimates of the isosteric heats of adsorption come from direct calorimetric measurements.[3−5] However, the apparatus needed for this purpose is not commercially available, and there is no known literature that investigates the temperature dependence of the isosteric heat of adsorption or the adsorbed-phase heat capacity using this approach. In contrast, the isosteric heat of adsorption is typically estimated by making certain assumptions and applying the Clausius−Clapeyron theory to adsorption isotherm data.[1] This approach relates the isosteric heat of adsorption to a temperature derivative of pressure on a logarithmic scale at constant loading. In turn, the adsorbed-phase heat capacity is related to the temperature derivative of the isosteric heat of adsorption and becomes equal to the gas-phase heat capacity when the temperature derivative of the isosteric heat of adsorption is zero. There are only two published approaches that look for possible dependencies of the isosteric heat of adsorption on temperature.

* Author to whom correspondence should be addressed. Phone: (803) 777-3590. Fax: (803) 777-8265. E-mail: ritter@engr.sc.edu.

Table 1. Summary of the Experimental Adsorption Equilibria of the *n*-Alkane Series C_1−C_7 on BAX-1100 Activated Carbon[13] and Adsorbate Thermodynamic Properties

adsorbate	P (Torr)	T (K)	N_p	T_c (K)	P_c (atm)	ω
methane	3.96−4964	293−343	302	190.6	45.398	0.008
ethane	0.08−4948	293−363	1063	305.4	48.162	0.098
propane	0.10−4953	293−363	909	369.8	41.944	0.152
n-butane	0.06−1494	293−363	871	425.2	37.503	0.193
n-pentane	0.07−100	293−363	812	469.6	33.259	0.251
n-hexane	0.06−100	293−363	394	507.4	29.312	0.296
n-heptane	0.15- 58	293−393	384	540.2	27.042	0.351

The first and more conventional approach depends on plotting the logarithm of the pressure versus the reciprocal of the temperature. This approach usually results in linear relationships,[1,6] leading to the assumption of a negligible temperature dependency. As an outcome, the adsorbed-phase heat capacity is conventionally approximated from the gas-phase heat capacity.[7] The second and more recent approach depends on fitting the adsorption equilibria to different pressure-explicit, temperature-dependent adsorption isotherm models and applying these models to the Clausius−Clapeyron equation to predict the isosteric heat of adsorption[2,8−11] and then the adsorbed-phase heat capacity from the implied and sometimes empirical temperature dependencies of the models. This approach, in general, shows that some adsorption conditions can cause slight temperature dependencies of the isosteric heat of adsorption, resulting in considerable relative deviations between the adsorbed- and gas-phase heat capacities. The adsorption conditions under which these deviations are most pronounced point, in most cases, to heavily adsorbed species, low temperatures, and high

10.1021/ie0004803 CCC: $20.00
Published on Web 12/08/2000

Table 2. Competing Predictors Used in the Stepwise Regression of ln(P)

1.0	n	n^2	n^3	n^{-1}	n^{-2}	n^{-3}	$\ln n$	$\ln n^2$	$\ln n^3$
T^{-1}	nT^{-1}	n^2T^{-1}	n^3T^{-1}	$n^{-1}T^{-1}$	$n^{-2}T^{-1}$	$n^{-3}T^{-1}$	$T^{-1}\ln n$	$T^{-1}\ln n^2$	$T^{-1}\ln n^3$
T^{-2}	nT^{-2}	n^2T^{-2}	n^3T^{-2}	$n^{-1}T^{-2}$	$n^{-2}T^{-2}$	$n^{-3}T^{-2}$	$T^{-2}\ln n$	$T^{-2}\ln n^2$	$T^{-2}\ln n^3$
T^{-3}	nT^{-3}	n^2T^{-3}	n^3T^{-3}	$n^{-1}T^{-3}$	$n^{-2}T^{-3}$	$n^{-3}T^{-3}$	$T^{-3}\ln n$	$T^{-3}\ln n^2$	$T^{-3}\ln n^3$
T	nT	n^2T	n^3T	$n^{-1}T$	$n^{-2}T$	$n^{-3}T$	$T\ln n$	$T\ln n^2$	$T\ln n^3$
T^2	nT^2	n^2T^2	n^3T^2	$n^{-1}T^2$	$n^{-2}T^2$	$n^{-3}T^2$	$T^2\ln n$	$T^2\ln n^2$	$T^2\ln n^3$
T^3	nT^3	n^2T^3	n^3T^3	$n^{-1}T^3$	$n^{-2}T^3$	$n^{-3}T^3$	$T^3\ln n$	$T^3\ln n^2$	$T^3\ln n^3$
$\ln T^{-1}$	$n\ln T^{-1}$	$n^2\ln T^{-1}$	$n^3\ln T^{-1}$	$\ln nT$	$\ln n^2T$	$\ln n^3T$	$\ln nT^{-1}$	$\ln n^2T^{-1}$	$\ln n^3T^{-1}$
$\ln T^{-2}$	$n\ln T^{-2}$	$n^2\ln T^{-2}$	$n^3\ln T^{-2}$	$\ln nT^2$	$\ln n^2T^2$	$\ln n^3T^2$	$\ln nT^{-2}$	$\ln n^2T^{-2}$	$\ln n^3T^{-2}$
$\ln T^{-3}$	$n\ln T^{-3}$	$n^2\ln T^{-3}$	$n^3\ln T^{-3}$	$\ln nT^3$	$\ln n^2T^3$	$\ln n^3T^3$	$\ln nT^{-3}$	$\ln n^2T^{-3}$	$\ln n^3T^{-3}$
$\ln T$	$n\ln T$	$n^2\ln T$	$n^3\ln T$	$\ln n^{-1}T^{-1}$	$\ln n^{-2}T^{-1}$	$\ln n^{-3}T^{-1}$			
$\ln T^2$	$n\ln T^2$	$n^2\ln T^2$	$n^3\ln T^2$	$\ln n^{-1}T^{-2}$	$\ln n^{-2}T^{-2}$	$\ln n^{-3}T^{-2}$			
$\ln T^3$	$n\ln T^3$	$n^2\ln T^3$	$n^3\ln T^3$	$\ln n^{-1}T^{-3}$	$\ln n^{-2}T^{-3}$	$\ln n^{-3}T^{-3}$			

Table 3. Most Significant[a] Predictors from the Stepwise Regression of the *n*-Alkane Series C_1−C_7 Adsorption Equilibria on BAX-1000 Activated Carbon[13] According to Equation 11[b]

i	c	v	t	i	c	v	t	i	c	v	t
	CH_4 (ARE = 5.12%)				C_3H_8 (ARE = 3.11%)				n-C_5H_{12} (ARE = 5.06%)		
1	−3.8601E+7	T^{-3}	−21.475	1	−9.1202E+7	T^{-3}	−203.85	1	−1.36816E+8	T^{-3}	−31.094
2	125.378	$T^{-1}\ln n^3$	7.268	2	0.278465	$\ln n^3T^{-1}$	43.172	2	0.837922	$\ln n^2T^{-1}$	24.396
3	−4.4251E+7	nT^{-3}	−6.855	3	3.68305E−8	T^3	41.673	3	5.83313E−08	T^2	20.496
4	4.69E+5	$n^{-1}T^{-3}$	6.512	4	84186	$T^{-2}\ln n$	40.478	4	12755	n^2T^{-2}	15.834
5	2.6857E+7	n^2T^{-3}	6.431	5	−60602.3	n^3T^{-3}	−14.950	5	−455167	n^3T^{-3}	−14.807
6	−5.154E+6	n^3T^{-3}	−5.272	6	667780	$n^{-1}T^{-3}$	13.328	6	8.785E+06	$T^{-3}\ln n^3$	9.478
7	−6.82E−5	n^{-2}	−4.160	7	0.026961	n^2	11.363	7	1.27533E−06	nT^2	6.376
8	1.12E−12	T^2n^{-3}	3.007	8	1.092E−3	nT	8.426	8	2.9208E+07	$n^{-1}T^{-3}$	5.008
9	−0.277249	$\ln n^{-1}T^{-3}$	−2.191	9	−4894.03	$n^{-2}T^{-3}$	−7.781	9	−66569	$n^{-1}T^{-2}$	−4.117
10	−1.892116	1	−0.826	10	28.842	$n^{-3}T^{-3}$	6.873		n-C_6H_{14} (ARE = 6.29%)		
	C_2H_6 (ARE = 7.72%)			11	−2.84581E−12	T^2n^{-3}	−6.589	1	−7.056646	$\ln n^{-1}T^{-3}$	−25.681
1	−61.743969	1	−68.140	12	−1.58956E−6	nT^2	−4.786	2	−136.065427	1	−25.237
2	−3.408468	$\ln n^{-1}\ T^{-3}$	−56.906		n-C_4H_{10} (ARE = 5.27%)			3	−6.94292E−08	T^3	−8.290
3	−0.002044	$T\ln n^3$	−32.575	1	−1.189E+8	T^{-3}	−47.746	4	−103139	n^3T^{-3}	−7.668
4	−1.51163E−7	T^3	−9.505	2	0.456012	$\ln n^3T^{-1}$	16.521	5	0.041075	Tn^{-1}	6.347
5	6.55963E−5	T^2	8.055	3	4.08185E−8	T^3	15.545	6	7704000	$T^{-3}\ln n^3$	5.274
6	807.228	$n^{-2}T^{-3}$	7.206	4	1.29E+7	$T^{-3}\ln n^2$	15.485	7	−6.99148E−5	T^2n^{-2}	−3.864
7	1.10198E−6	n^2T^2	6.983	5	−1.09	n^3T^{-1}	−14.627	8	2.14215E−5	T^2n^{-3}	2.954
8	−9.57822	$n^{-3}T^{-3}$	−6.228	6	4.42045E−7	n^2T^2	10.728		n-C_7H_{16} (ARE = 12.22%)		
9	−2.09288E−7	T^2n^{-1}	−6.029	7	76.366	nT^{-1}	8.808	1	−1595.12	T^{-1}	−16.837
10	2.57E−2	$n^{-3}T^{-2}$	5.868	8	−1.1956E−6	nT^2	−3.306	2	1.04049E−5	nT^2	16.202
11	−2.527E−4	n^2T	−5.203	9	240425	$n^{-2}T^{-3}$	3.228	3	−3.23065E+8	$n^{-1}T^{-3}$	−14.661
12	5.4559E−5	Tn^{-1}	4.541	10	−2.94356E−8	T^2n^{-2}	−2.494	4	1.314E+8	$n^{-2}T^{-3}$	7.196
				11	−3.95291E−7	$T^2\ln n^2$	−1.649	5	−2.3094E+7	$n^{-3}T^{-3}$	−5.283
								6	−2.32454E−6	$T^2\ln n^2$	−3.902

[a] Largest absolute values of t that satisfied the acceptance criteria. [b] P, T, and n are in atm, Kelvin, and mol/kg, respectively.

loadings. These are also the conditions under which the two main assumptions in the Clausius−Clapeyron equation, i.e., ideal gas and negligible adsorbed-to-gas-phase specific volume ratio, tend to become less valid,[12] with the ideal-gas assumption being the most severe.

The objective of this study is to further evaluate these two approaches, and also to evaluate some of the assumptions involved, by applying to the extensive experimental isotherm data set presented in Part 1 of this series[13] a new model based on a statistically optimized regression method and also a virial-type pressure-explicit isotherm model. Specifically, the experimental adsorption equilibria obtained for the normal alkane series C_1−C_7 over a wide range of temperatures and pressures[13] on Westvaco BAX-1100 activated carbon (see Table 1) is correlated with these two models. Both models give rise to explicit expressions for the isosteric heat of adsorption, and the difference between the differential adsorbed- and molar gas-phase heat capacities. Therefore, the corresponding isosteric heats of adsorption and adsorbed-phase heat capacities are predicted from these expressions and compared to each other under different adsorption conditions. The effect of assuming ideal-gas behavior in the Clausius−Clapeyron equation on predicting the isosteric heat of adsorption and the adsorbed-phase heat capacity is also evaluated and discussed. The temperature-independent isosteric heats of adsorption predicted from the potential theory model correlation developed in Part 1 of this series[13] are also compared with those predicted from the statistically optimized and virial-type models; similarities and differences are noted.

Theory

Isosteric Heat of Adsorption and Adsorbed-Phase Heat Capacity. The isosteric heat of adsorption is typically determined with the assumptions of ideal-gas behavior and negligible ratio of adsorbed-to-gas-phase specific volumes, which leads to the Clausius−Clapeyron equation[12]

$$q^{(\mathrm{IG})} = RT^2\left(\frac{\partial \ln P}{\partial T}\right)_n \tag{1a}$$

or, alternatively

$$q^{(\mathrm{IG})} = -R\left(\frac{\partial \ln P}{\partial (1/T)}\right)_n \tag{1b}$$

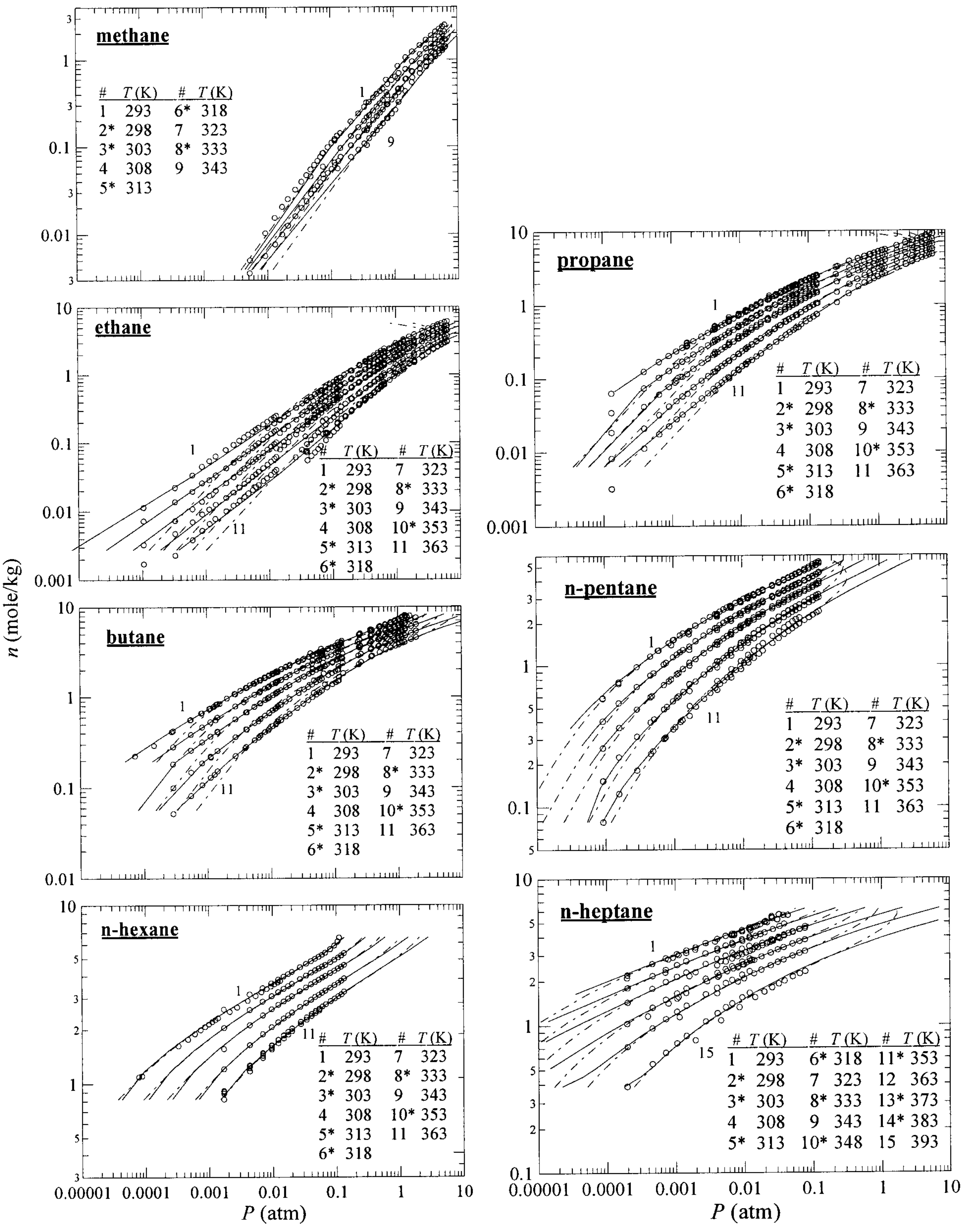

Figure 1. Representative adsorption equilibria for the n-alkane series C_1-C_7 on BAX-1100 activated carbon. Symbols represent experimental data,[13] and solid and dash−dotted lines, respectively, represent SW and VT correlations. Numbers with asterisks indicate temperatures available in the experimental data set and accounted for in the calculations but not shown on these plots.

where R, P, T, and n denote the universal gas constant,equilibrium pressure, absolute temperature, and amount adsorbed, respectively, and the superscript (IG) refers to the ideal-gas assumption. At high pressures or for large molecules, the ideal-gas assumption becomes invalid, and the isosteric heat of adsorption from the Clausius−Clapeyron equation, assuming a negligible adsorbed-to-gas-phase specific volume ratio, reduces to

$$q = zq^{(IG)} \tag{2}$$

where z is the real-gas compressibility factor at P and T, which is readily obtained from an appropriate equation of state.

Table 4. Virial Model Regression Parameters for the *n*-Alkane Series C_1−C_7 Adsorption Equilibria on BAX-1100 Activated Carbon[13]

variable	CH_4	C_2H_6	C_3H_8	n-C_4H_{10}	n-C_5H_{12}	n-C_6H_{14}	n-C_7H_{16}
$A^{(0)}$	6.927	7.680	17.020	7.294	6.109	9.537	21.878
$A^{(1)}$ (K)	−1723	−3155	−10034	−4268	−4641	−6467	−15861
$A^{(2)}$ (K^2)	−94538	415	1033248	−7300	2365	75756	1569960
$B^{(0)}$ (m^2/mol)	−5382794	1545807	−3259566	361234	5219271	369185	−142661
10^{-9} $B^{(1)}$ (K m^2/mol)	3.604	−0.337	2.773	0.121	−2.172	0.268	1.264
$10^{-10}B^{(2)}$ (K^2 m^2/mol)	−55.835	2.689	−47.647	0.424	28.026	0.273	−22.657
10^{-12} $C^{(0)}$ (m^4/mol^2)	−0.645	−2.528	−0.141	0.093	−3.383	−0.051	−0.676
10^{-15} $C^{(1)}$ (K m^4/mol^2)	0.058	1.294	−0.085	−0.109	1.801	−2.8E−4	0.228
10^{-17} $C^{(2)}$ (K^2 m^4/mol^2)	0.277	−1.722	0.316	0.170	−2.470	0	−0.226
ARE (%)	8.67	30.26	18.15	10.76	6.19	6.39	11.23

A virial-type equation of state with the Pitzer generalized second virial coefficient correlation[14] is used here for calculating the compressibility factor

$$z = 1 + (B_G^{(0)} + \omega B_G^{(1)})\left(\frac{P_r}{T_r}\right) + ... \qquad (3)$$

where ω is the accentric factor and P_r and T_r are the reduced pressure and temperature, respectively. The pressure in this equation is obtained from the corresponding adsorption isotherm as a function of temperature and the amount adsorbed. $B_G^{(0)}$ and $B_G^{(1)}$ are coefficients of the gas-phase second virial coefficient and can be estimated accurately at low-to-moderate pressures or moderate-to-high temperatures from[14]

$$B_G^{(0)} = 0.083 - \frac{0.422}{T_r^{1.6}} \qquad (4)$$

$$B_G^{(1)} = 0.139 - \frac{0.172}{T_r^{4.2}} \qquad (5)$$

Al-Muhtaseb and Ritter[2] showed that the deviation between the differential adsorbed- and molar gas-phase heat capacities (ideal-gas behavior) can be estimated from the temperature dependence of the isosteric heat of adsorption as

$$\Delta\bar{C}p_a^{(IG)} = \bar{C}p_a^{(IG)} - \tilde{C}p_g = -\left(\frac{\partial q^{(IG)}}{\partial T}\right)_n \qquad (6)$$

or as

$$\Delta\bar{C}p_a = \bar{C}p_a - \tilde{C}p_g = -\left(\frac{\partial q}{\partial T}\right)_n = z\Delta\bar{C}p_a^{(IG)} - q^{(IG)}\left(\frac{\partial z}{\partial T}\right)_n \qquad (7)$$

when real-gas behavior is considered. Differentiating eqs 3−5 with respect to temperature and substituting eq 1 for the temperature derivative of pressure gives

$$\left(\frac{\partial z}{\partial T}\right)_n = \left[\frac{1}{T_c}\left(\frac{0.6752}{T_r^{2.6}} + \frac{0.7224}{T_r^{5.2}}\omega\right) - \frac{(B_G^{(0)} + \omega B_G^{(1)})}{T}\left(1 - \frac{q^{(IG)}}{RT}\right)\right]\left(\frac{P_r}{T_r}\right) \qquad (8)$$

The deviation between the molar adsorbed- and gas-phase heat capacities includes contributions from the deviation between the differential adsorbed- and molar gas-phase heat capacities as well as the spreading pressure.[2] This deviation is, therefore, estimated from

$$\Delta\tilde{C}p_a^{(IG)} = \tilde{C}p_a^{(IG)} - \tilde{C}p_g = \frac{1}{n}\int_0^n\left[\Delta\bar{C}p_a^{(IG)} + R\left(\frac{\partial(\ln P + q^{(IG)}/RT)}{\partial \ln n}\right)_T\right]\partial n \qquad (9)$$

$$\Delta\tilde{C}p_a = \tilde{C}p_a - \tilde{C}p_g = \frac{1}{n}\int_0^n\left[\Delta\bar{C}p_a + R\left(\frac{\partial(\ln P + q/RT)}{\partial \ln n}\right)_T\right]\partial n \qquad (10)$$

where eq 9 represents the ideal-gas behavior[2] and eq 10 represents the real-gas behavior. The integrals in eqs 9 and 10 can be evaluated numerically using results from the adsorption isotherms and the corresponding ideal-gas and real-gas isosteric heats of adsorption and adsorbed-phase heat capacities.

Derived Thermodynamic Properties from the Stepwise (SW) Regression Model. The idea of using stepwise (SW) regression[15−17] is to find only those variables that make a significant contribution in correlating the objective variable. This is achieved by sequentially adding and deleting covariates one by one until all of the important predictors (variables) are kept in the final model and all of the unimportant ones are left out. The most effective variables are those that cause the largest values of variances to produce the least sum squared errors. The efficacy of the variables is indicated by the relative magnitudes of the absolute t values through the analysis of variance (ANOVA) of the final correlation.

In this study, the 121 predictors listed in Table 2 are allowed to compete statistically in correlating ln P according to the following equation:

$$\ln P = \sum_i c_i v_i \qquad (11)$$

where v_i is the competing predictor (variable) and c_i is the corresponding coefficient (constant). Only the predictors that provide a predetermined minimum degree of contribution (i.e., that pass the t test by scoring an absolute t parameter that is greater than or equal to a set minimum value) survive the competition. This method thus gives a fair representation of the experimental isotherm data without any interference from the form of the proposed model. However, depending on the resulting form of eq 11, this method might give rise to nonzero pressures as $n \rightarrow 0$, which is not thermodynamically consistent. Nevertheless, this is not a major concern because, if it does occur, it only affects the results at exceedingly low pressures and in this region the effects are considered minimal, as they are in potential theory models, which suffer from essentially the same thermodynamic inconsistency.[18,19]

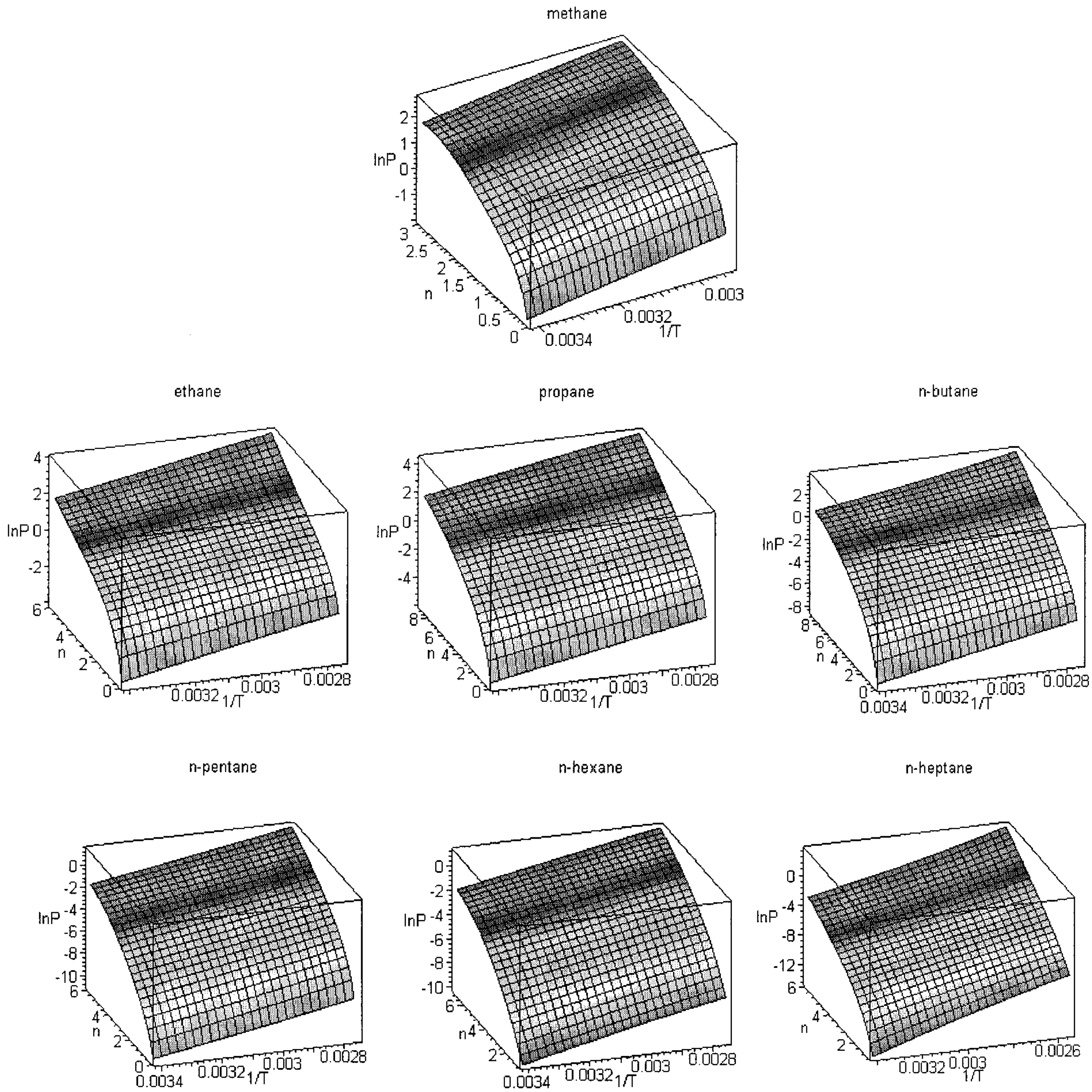

Figure 2. Clausius−Clapeyron representation of ln(P) dependence on 1/T and loading (n) based on results from the SW correlation.

By substituting the final SW correlation into eqs 1 and 5, the following expressions are obtained for the isosteric heat of adsorption and the deviation between the differential adsorbed- and molar gas-phase heat capacities, respectively:

$$q_{\mathrm{SW}}^{(\mathrm{IG})} = RT^2\sum_i c_i\left(\frac{\partial v_i}{\partial T}\right)_n \tag{12}$$

$$\Delta\bar{C}\mathrm{p}_{\mathrm{a,SW}}^{(\mathrm{IG})} = -RT\left[2\sum_i c_i\left(\frac{\partial v_i}{\partial T}\right)_n + T\sum_i c_i\left(\frac{\partial^2 v_i}{\partial T^2}\right)_n\right] \tag{13}$$

The deviation between the molar adsorbed- and gas-phase heat capacities is estimated by evaluating the integral in eq 9 numerically using results from eqs 11−13 or analytically if the predictors that pass the t test are not too complicated for evaluating the needed integrations.

Derived Thermodynamic Properties from the Virial-Type (VT) Adsorption Isotherm. The virial-type (VT) adsorption isotherm[20] is usually truncated after the third virial coefficient and given by

$$\ln\left(\frac{P}{n}\right) = A + 2B\left(\frac{n}{a}\right) + \frac{3}{2}C\left(\frac{n}{a}\right)^2 + ... \tag{14}$$

where a is the adsorbent specific surface area and A, B, and C are the first, second, and third virial coefficients, respectively. These coefficients were shown to follow the following temperature dependence:[20]

$$\{A, B, C, ...\} = \sum_{i=0}^{m}\frac{\{A^{(i)}, B^{(i)}, C^{(i)}, ...\}}{T^i} \tag{15}$$

with values of m equal to 1 or 2. This and another form of the VT model were successfully used to derive the isosteric heat of adsorption for single- and mixed-gas adsorption.[9,21] It gave thermodynamically consistent analytical models and showed a promising performance, especially for predictions of the derived thermodynamic properties for an unlimited number of components using only single-component adsorption isotherm parameters.

Moreover, it was also shown that raising the value of m from 1 to 2 significantly improves the models ability to correlate the equilibrium isotherm data and also reveals an overlooked temperature dependency of the isosteric heat of adsorption.

Substituting eqs 14 and 15 into eq 1 gives the following expression for the isosteric heat of adsorption:

$$q_{\mathrm{VT}}^{(\mathrm{IG})} = -R\left[\sum_{i=0}^{m}\frac{iA^{(i)}}{T^{i-1}} + 2\left(\sum_{i=0}^{m}\frac{iB^{(i)}}{T^{i-1}}\right)\left(\frac{n}{a}\right) + \frac{3}{2}\left(\sum_{i=0}^{m}\frac{iC^{(i)}}{T^{i-1}}\right)\left(\frac{n}{a}\right)^2 + ...\right] \quad (16)$$

Equation 16 gives a temperature dependence on the order of $T^{(1-m)}$. Therefore, substituting it into eq 6 gives

$$\Delta\bar{C}\mathrm{p}_{\mathrm{a,VT}}^{(\mathrm{IG})} = -R\left[\frac{q_{\mathrm{VT}}^{(\mathrm{IG})}}{RT} + \sum_{i=0}^{m}\frac{i^2A^{(i)}}{T^i} + 2\left(\sum_{i=0}^{m}\frac{i^2B^{(i)}}{T^i}\right)\left(\frac{n}{a}\right) + \frac{3}{2}\left(\sum_{i=0}^{m}\frac{i^2C^{(i)}}{T^i}\right)\left(\frac{n}{a}\right)^2 + ...\right] \quad (17)$$

which reduces to zero when $m = 1$. Substituting eqs 14–17 into eq 9 gives the following analytic expression for the deviation between the molar adsorbed- and gas-phase heat capacities:

$$\Delta\tilde{C}\mathrm{p}_{\mathrm{a,VT}}^{(\mathrm{IG})} = R\left[1 + \sum_{i=0}^{m}\frac{iA^{(i)}}{T^i} - \sum_{i=0}^{m}\frac{i^2A^{(i)}}{T^i} + \left(\sum_{i=0}^{m}\frac{B^{(i)}}{T^i} - \sum_{i=0}^{m}\frac{i^2B^{(i)}}{T^i}\right)\left(\frac{n}{a}\right) + \left(\sum_{i=0}^{m}\frac{C^{(i)}}{T^i} - \sum_{i=0}^{m}\frac{iC^{(i)}}{2T^i} - \sum_{i=0}^{m}\frac{i^2C^{(i)}}{2T^i}\right)\left(\frac{n}{a}\right)^2 + ...\right] \quad (18)$$

The spreading pressure contribution in eq 18 is estimated by substituting $m = 1$, which eliminates the effect of temperature on the isosteric heat of adsorption and gives

$$\Delta\tilde{C}\mathrm{p}_{\mathrm{a,VT}}^{(\mathrm{IG})} = R\left[1 + B^{(0)}\left(\frac{n}{a}\right) + C^{(0)}\left(\frac{n}{a}\right)^2 + ...\right] \quad (19)$$

Results and Discussion

Correlation of Adsorption Equilibria. The experimental adsorption isotherms[13] were regressed using the stepwise (SW) regression method[8] according to eq 11 with the least sum square error (LSSE) in ln(P) as the objective function. An entry and removal of F probabilities of 5 and 10%, respectively, were used to obtain the optimum set of predictors for each system. These optimum sets of predictors are listed in Table 3, along with the corresponding t values. Typically, 6–12 predictors survived the competition, depending on the n-alkane. The absolute magnitude of a t value indicates qualitatively the extent of its contribution to the final regressed formula, wherein higher absolute values are statistically more effective in the overall description. Because the SW method is also considered a hybrid of forward selection (FWD) and backward rejection (BWD) methods, the same data were also fitted to these two methods; the results are presented in Tables A1 and A2, respectively (see the Appendix). Overall, the SW method had a major advantage over both the FWD and BWD methods in producing more concise correlations with significantly lower average relative errors. Therefore, neither the FWD nor the BWD results were used in this work to derive any thermodynamic properties. The experimental adsorption isotherms were also regressed to the virial-type model with $m = 2$ according to eqs 14 and 15 using the LSSE in ln(P/n) as the objective function. The percent average relative errors (AREs) in pressure from each model were used to indicate the goodness of the resulting correlations; they were calculated from

$$\mathrm{ARE} = \frac{100\%}{N_{\mathrm{p}}}\sum_{i=1}^{N_{\mathrm{p}}}\frac{|P_i^{\mathrm{exp}} - P_i^{\mathrm{corr}}|}{P_i^{\mathrm{exp}}} \quad (20)$$

where N_{p} is the number of experimental data points, which is given in Table 1 for each data set, and the superscripts exp and corr denote experimental and correlated pressures, respectively. Representative results from both models are plotted versus the experimental data in Figure 1; the corresponding correlation parameters and AREs are given in Tables 3 and 4 for the SW and VT models, respectively.

Although the AREs from the SW and VT models were almost the same, it is clear from Figure 1 that the SW correlations provided a slightly more reliable representation of the experimental data, especially in the high-pressure region where the VT model isotherms indicated an unrealistic inversion in the equilibrium pressures beyond the maximum experimental value of the amount adsorbed. The amounts adsorbed at very low pressures were also very often slightly underestimated by the VT model. Therefore, the SW model was considered to be more suitable for interpolation and extrapolation of the experimental adsorption equilibria. Hence, the SW model correlations were used here as an alternative to the conventional numerical differentiation of the equilibrium isotherm data according to the Clausius–Clapeyron equation to explore the temperature dependence of the isosteric heat of adsorption.

Figure 2 shows the pressure logarithm, ln(P) (P in atm), as represented by the SW method, versus the amount adsorbed, n, and the reciprocal temperature, $1/T$. This is the more common method that is used to indirectly estimate the isosteric heat of adsorption.[1,6] In this form, ln(P) was easily visualized to have an almost perfect linear dependence on $1/T$ at any fixed value of n, thereby indicating that the isosteric heat of adsorption was independent of temperature. However, the SW statistical analysis of the various forms of temperature dependencies of ln(P) shown in Table 3 reveal that the $1/T$ dependence hardly provided any significant contribution to ln(P) relative to higher orders of temperature dependencies and that the $1/T$ dependence passed the t test only occasionally with low values. Moreover, the statistically significant predictors listed in Table 3 show that the temperature dependence became increasingly more complicated for the more heavily adsorbed alkanes.

Prediction of the Isosteric Heat of Adsorption. The SW and VT correlations were used to predict the isosteric heat of adsorption according to eq 1, which assumes ideal-gas behavior, and according to eq 2, which corrects for nonideal-gas behavior with the

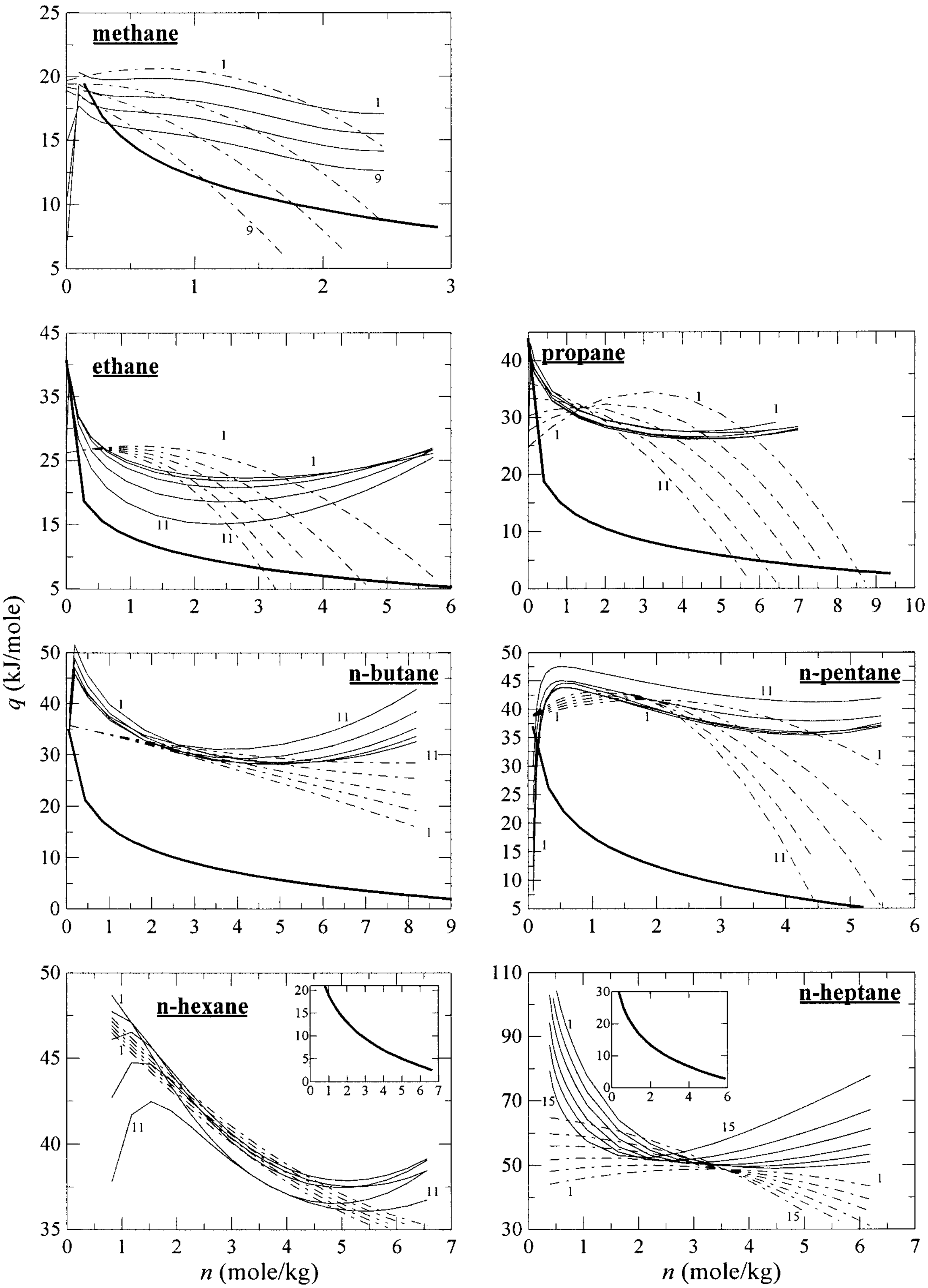

Figure 3. Isosteric heats of adsorption for the *n*-alkane series C_1-C_7 on BAX-1100 activated carbon predicted from the ideal-gas formulas derived from the SW (thin solid lines), VT (dash−dotted lines), and potential theory (thick solid lines) models. Temperatures are numbered as in Figure 1.

compressibility factor. Figure 3, which compares the predictions from the SW and VT models utilizing the ideal-gas assumption, shows that the predicted isosteric heats of adsorption from both the SW and the VT models were all in the same range, except at very high amounts adsorbed. However, the SW predictions exhibited a more uniform dependence over the entire range of the amount adsorbed, except near zero coverage of the lightly adsorbed components. The noticeable artifacts at zero coverage were expected because of the aforementioned thermodynamic inconsistency of the SW model in this region. The VT model also gave almost the same temperature dependence as the SW model, but only at low-to-moderate amounts adsorbed of the light components (such as methane) and only at moderate amounts adsorbed of the moderate-to-heavy components. However, the VT model rarely agreed with the SW model at very high amounts adsorbed, most likely because the VT model misrepresented the adsorption equilibria at extremely high pressures, as shown in Figure 1. Overall,

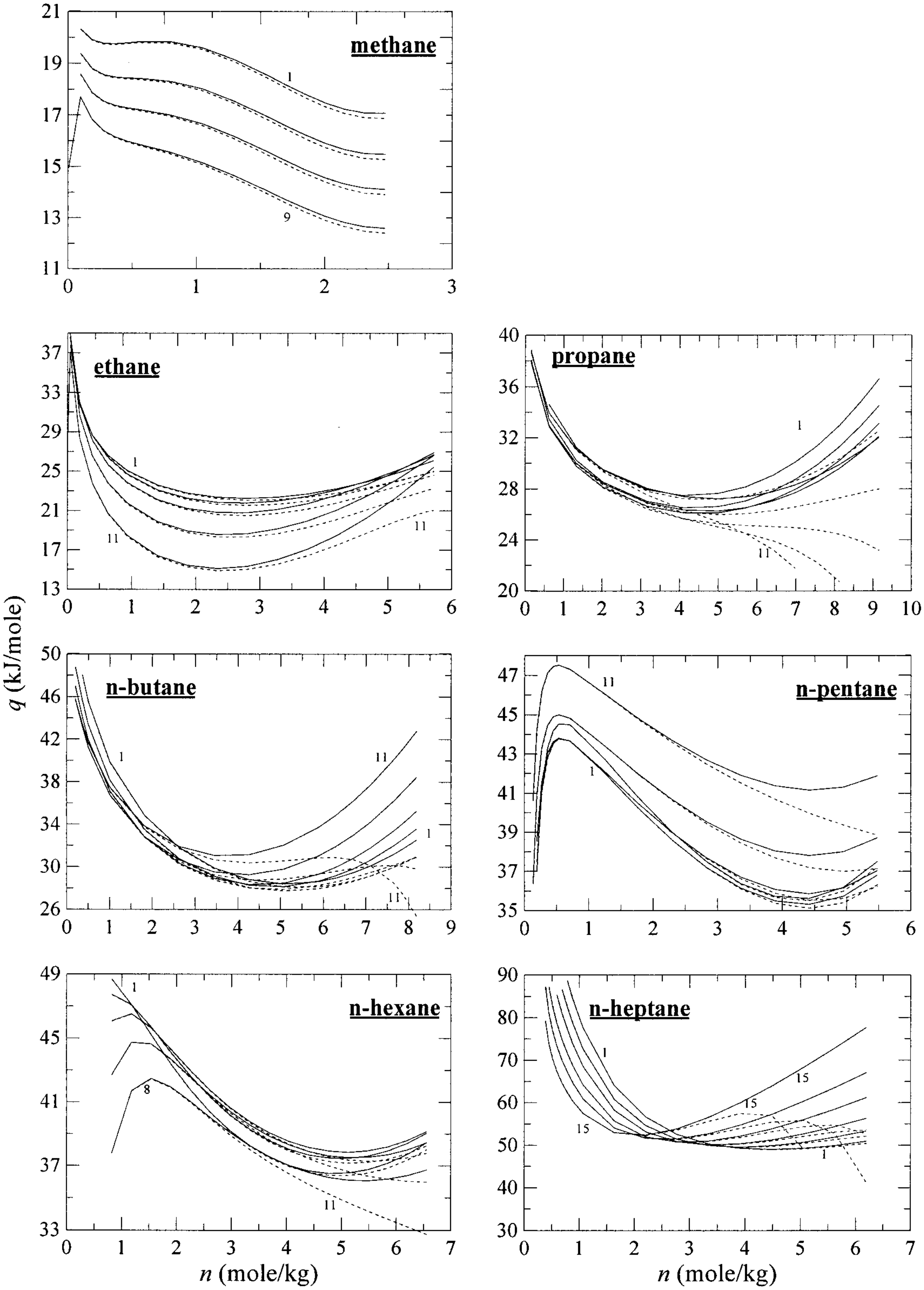

Figure 4. Comparison of real-gas (dash−dotted lines) with ideal-gas (solid lines) isosteric heats of adsorption for the *n*-alkane series C_1-C_7 on BAX-1100 activated carbon predicted from the corresponding formulas from the SW model. Temperatures are numbered as in Figure 1.

the temperature dependence of the isosteric heat of adsorption was relatively slight, especially over narrow ranges of temperature and for relatively lightly adsorbed components.

Figure 3 also compares the temperature-dependent isosteric heats of adsorption predicted from the SW and VT models to the temperature-independent isosteric heat of adsorption obtained from the potential theory characterestic curve developed in Part 1 of this series.[13]

The potential theory isosteric heat of adsorption was obtained by applying the Clausius−Clapeyron equation to the general characterestic curve presented in Part 1,[13] which gives

$$q^{(\mathrm{IG})} = \frac{R}{62396}\beta v\left[-1.458 \times 10^{7} \ln\left(\frac{nv}{825.421}\right)\right]^{0.821283} \tag{21}$$

where n and v are, respectively, the amount adsorbed

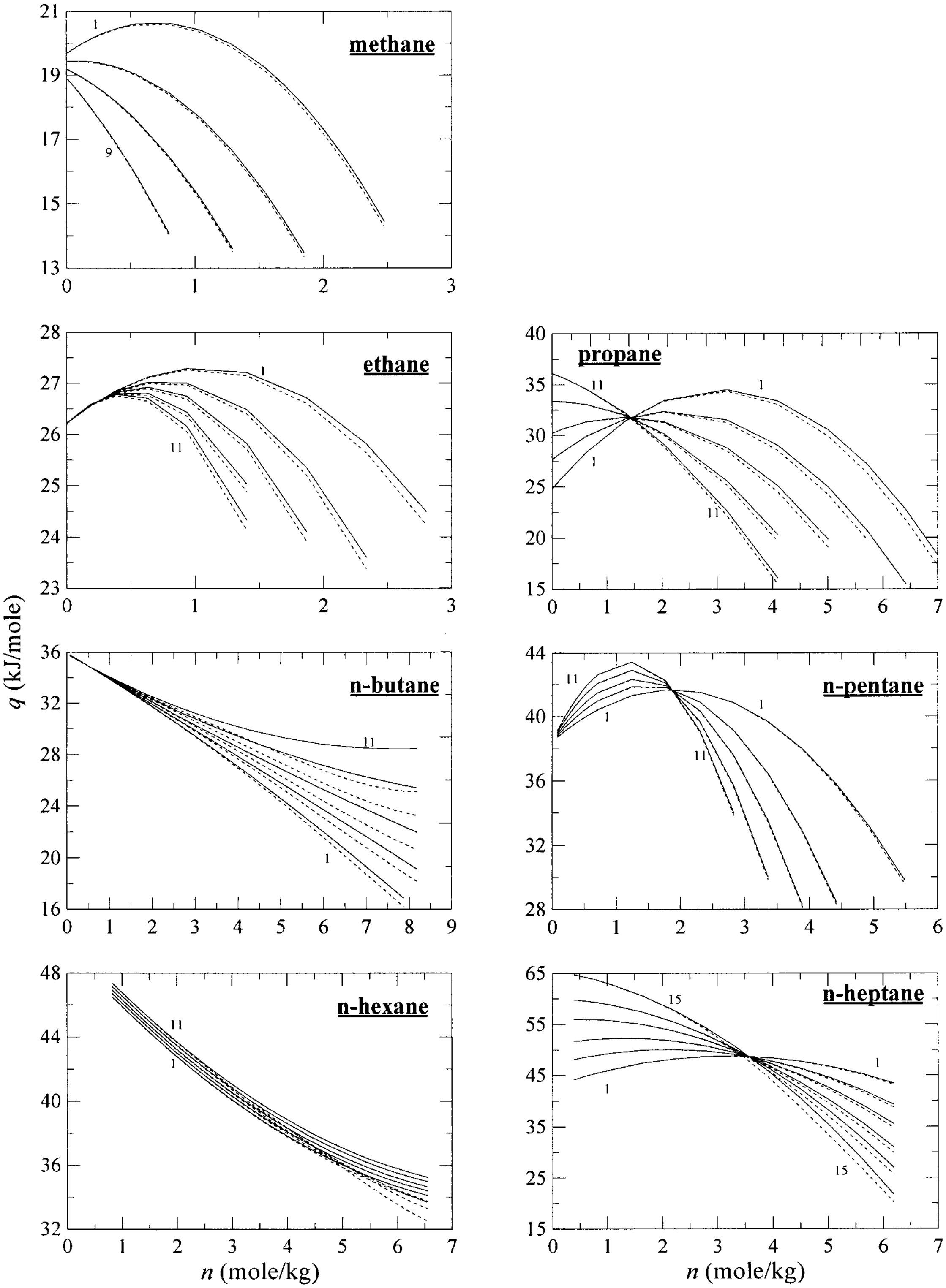

Figure 5. Comparison of real-gas (dash−dotted lines) with ideal-gas (solid lines) isosteric heats of adsorption for the *n*-alkane series C_1-C_7 on BAX-1100 activated carbon predicted from the corresponding formulas from the VT model. Temperatures are numbered as in Figure 1.

(in moles per kilogram) and the specific volume (in cubic centimeters per mole) of the liquid phase at the normal boiling point of the corresponding *n*-alkane.[13] R is the universal gas constant (8.314×10^{-3} kJ mol^{-1} K^{-1}), and β is the coalescing factor for each *n*-alkane.[13] The temperature-independent potential theory isosteric heat of adsorption agrees well with the average SW and VT isosteric heats of adsorption for lightly to moderately adsorbed components at low amounts adsorbed and with the VT model for lightly to moderately adsorbed components at high amounts adsorbed. However, the potential theory isosteric heat of adsorption dramatically underestimates the SW and VT isosteric heats of adsorption predicted under other conditions and for heavily adsorbed components like *n*-hexane and *n*-heptane. In such cases, it tended to be nearer to the SW and VT predictions at relatively high temperatures, possibly because of the nature of the potential theory

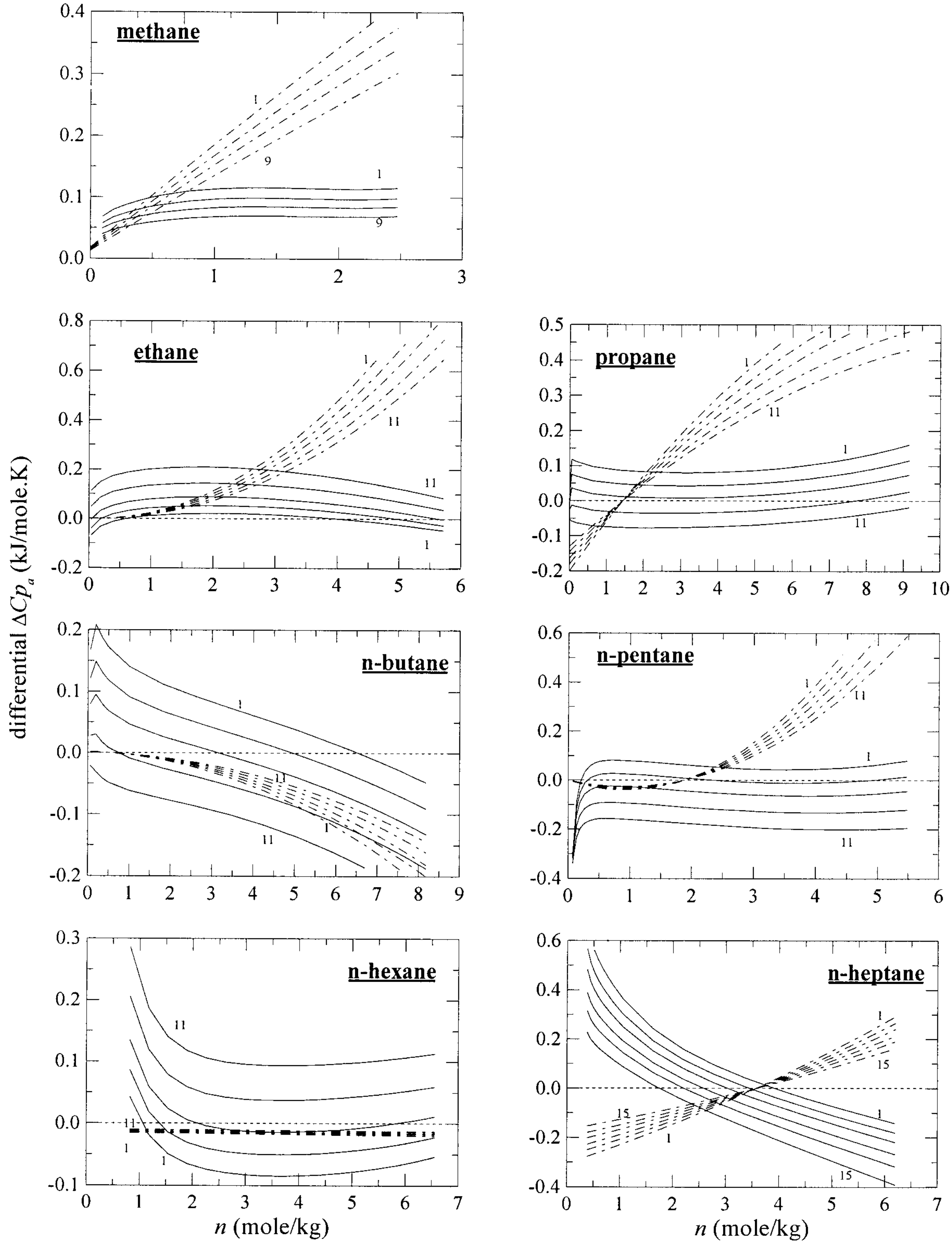

Figure 6. Deviations between the differential adsorbed- and molar gas-phase heat capacities for the n-alkane series C_1–C_7 on BAX-1100 activated carbon predicted from the ideal-gas formulas derived from the SW (solid lines) and VT (dash–dotted lines) models. Temperatures are numbered as in Figure 1.

model being more applicable to the lightly adsorbed species and very low relative pressures.[13]

Figures 4 and 5 show that after both models are corrected for real-gas behavior according to eq 2, the differences in the isosteric heats of adsorption based on ideal- and real-gas versions of the Clausius–Clapeyron equation were apparent only for high loadings and relatively heavily adsorbed components. However, the deviations from the SW model predictions were more pronounced than those from the VT model. This result was possibly related to the unrealistic inversion of the pressure estimated from the VT model, as shown in Figure 1. Because the VT model underestimated the equilibrium pressures severely at very high loadings, the calculated pressure necessarily (but falsely) indicated close-to-ideal-gas conditions at such loadings.

It is also shown in Figure 4, and to a lesser extent in Figure 5, that the deviations between the ideal- and

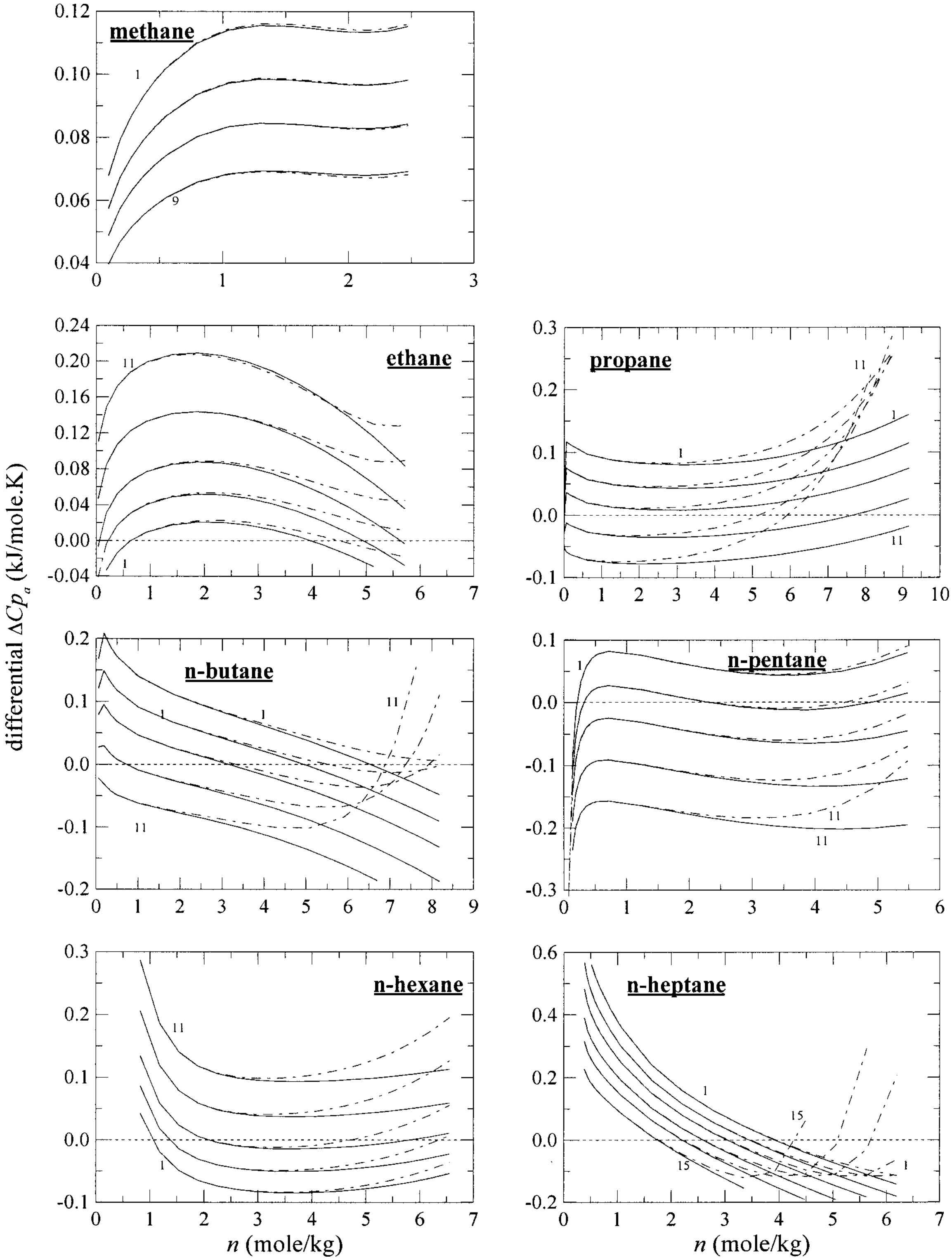

Figure 7. Comparison of real-gas (dash−dotted lines) with ideal-gas (solid lines) deviations between the differential adsorbed- and molar gas-phase heat capacities for the *n*-alkane series C_1−C_7 on BAX-1100 activated carbon predicted from the corresponding formulas derived from the SW model. Temperatures are numbered as in Figure 1.

real-gas isosteric heats of adsorption were most pronounced at both high loadings and high temperatures. Although it is generally understood that high temperatures in the gas phase promote ideality, in isosteric adsorption equilibria, high temperatures correspond to high pressures in the gas phase to achieve the required amount adsorbed; this effectively demotes ideality at high temperatures in this case. Overall, correcting the predictions from both models for real-gas behavior reduced the isosteric heats of adsorption relative to those based on ideal-gas behavior, especially at high loadings. These results agree with those obtained from density functional theory.[12]

Prediction of the Adsorbed-Phase Heat Capacity. Figure 6 compares the deviations between the differential adsorbed- and molar gas-phase heat capacities predicted from the SW and VT models utilizing the ideal-gas assumption. Again, the SW model was more

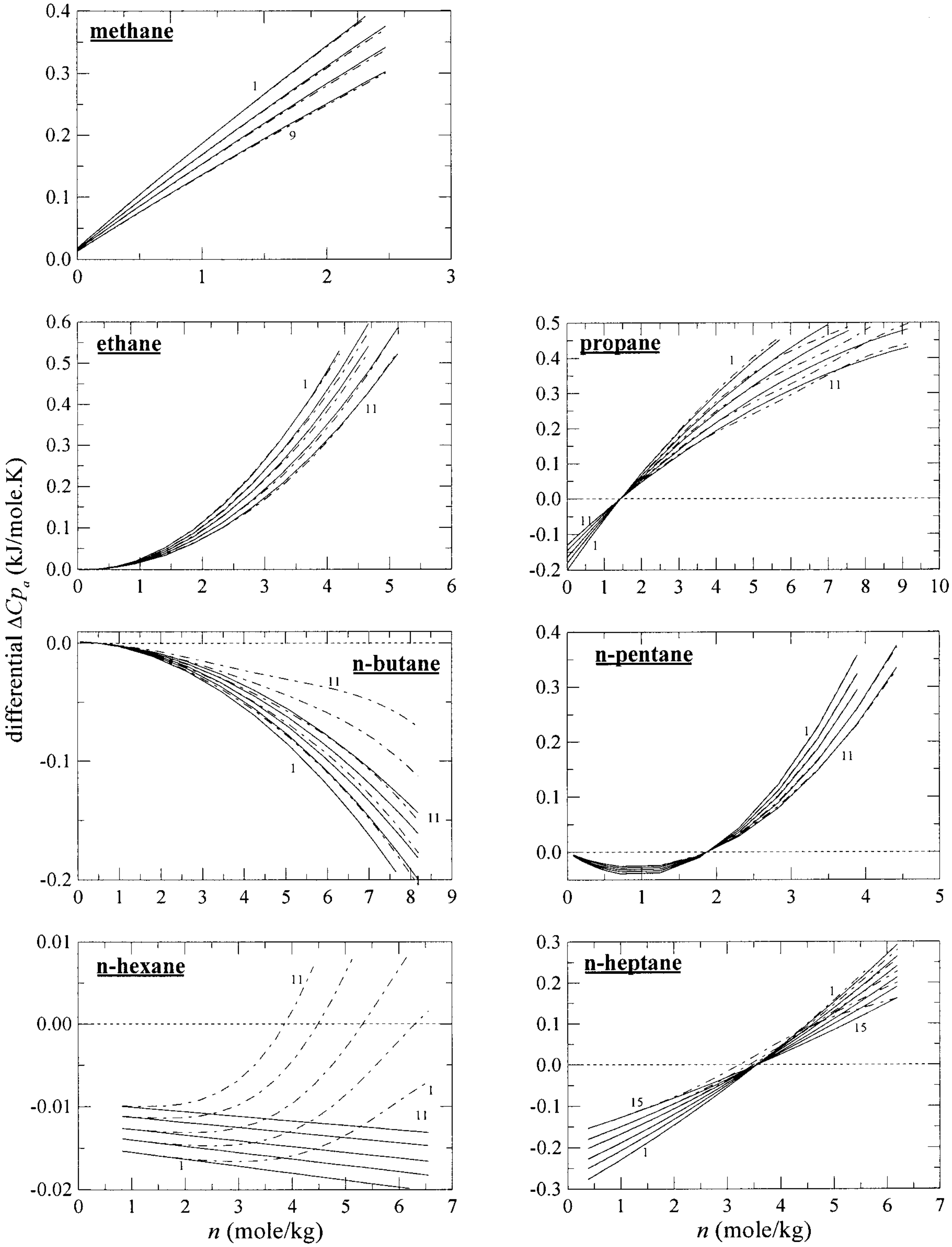

Figure 8. Comparison of real-gas (dash−dotted lines) with ideal-gas (solid lines) deviations between the differential adsorbed- and molar gas-phase heat capacities for the n-alkane series C_1−C_7 on BAX-1100 activated carbon predicted from the corresponding formulas derived from the VT model. Temperatures are numbered as in Figure 1.

stable in its predictions than the VT model, which tended to overestimate the deviations at very high loadings. In contrast, the SW model always exhibited finite deviations between the differential adsorbed- and molar gas-phase heat capacities at very high loadings, in agreement with results shown elsewhere.[2] For low-to-moderate loadings of the lightly adsorbed species and for moderate loadings of the relatively heavily adsorbed species, both models predicted similar trends in the deviations. Overall, the deviations between the differential adsorbed- and molar gas-phase heat capacities were strongly dependent on the amounts adsorbed and weakly dependent on temperature, also in agreement with results reported elsewhere.[2]

The real-gas correction to the predicted deviations between the differential adsorbed- and molar gas-phase heat capacities were again more apparent with the SW model than with the VT model, as shown in Figures 7

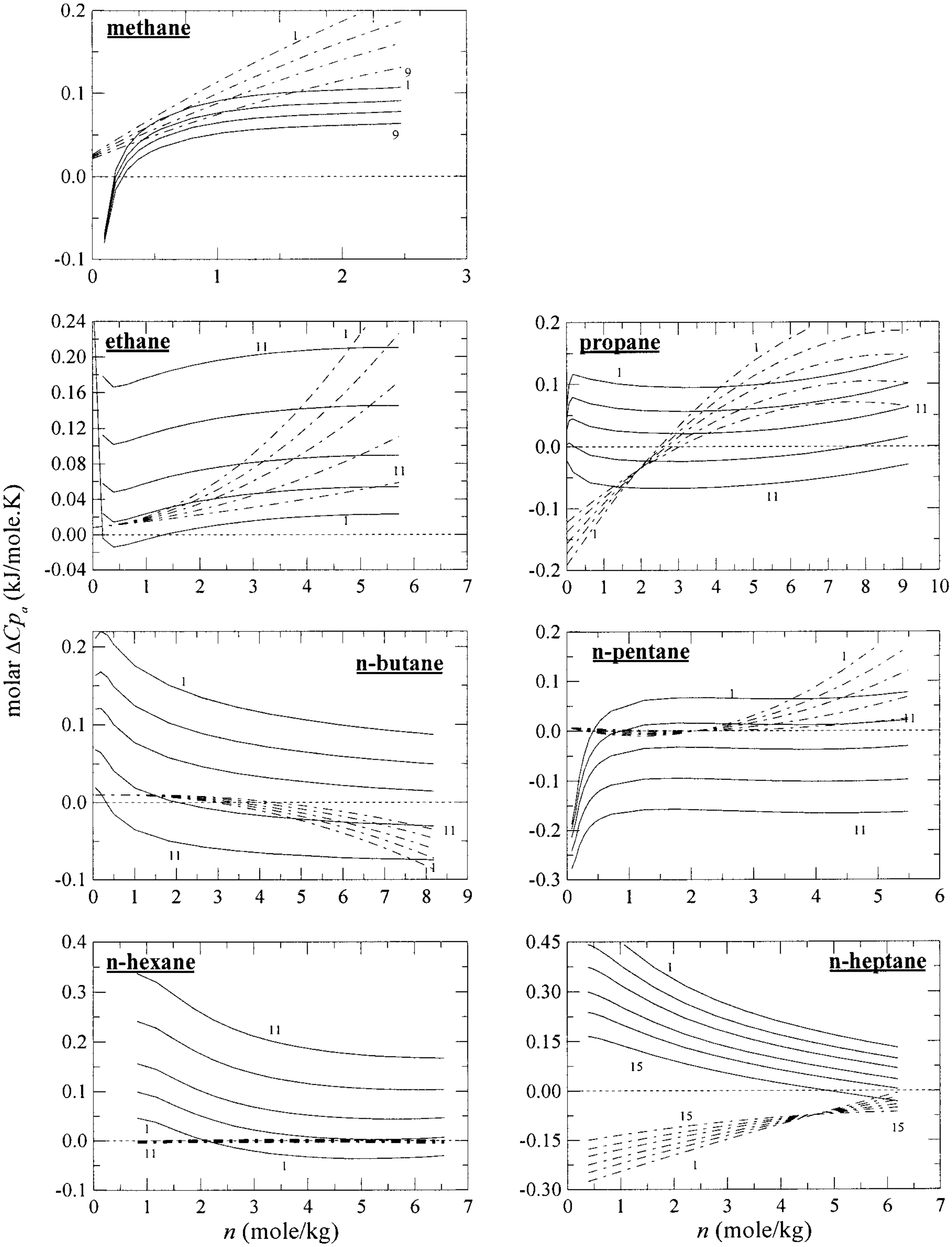

Figure 9. Deviations between the molar adsorbed- and gas-phase heat capacities for the *n*-alkane series C_1-C_7 on BAX-1100 activated carbon predicted from the ideal-gas formulas derived from the SW (solid lines) and VT (dash−dotted lines) models. Temperatures are numbered as in Figure 1.

and 8, respectively. The corrections were also more pronounced at high loadings and, to a lesser extent, at high temperatures. However, the real-gas corrections sometimes predicted erroneously high deviations between the differential adsorbed- and molar gas-phase heat capacities at very high amounts adsorbed, as shown for heptane in Figure 7.

Figure 9 shows the deviations between the molar adsorbed- and gas-phase heat capacities. Overall, the same trends as shown in Figure 6 are noticed here but with a relatively wider range of agreement between the SW and VT models, possibly because of the contribution of the spreading pressure term in eqs 9 and 10. The sometimes erroneously high deviations between the differential adsorbed- and molar gas-phase heat capacities observed with the real-gas corrections shown in Figure 7 are less apparent in the deviations between the molar adsorbed- and gas-phase heat capacities

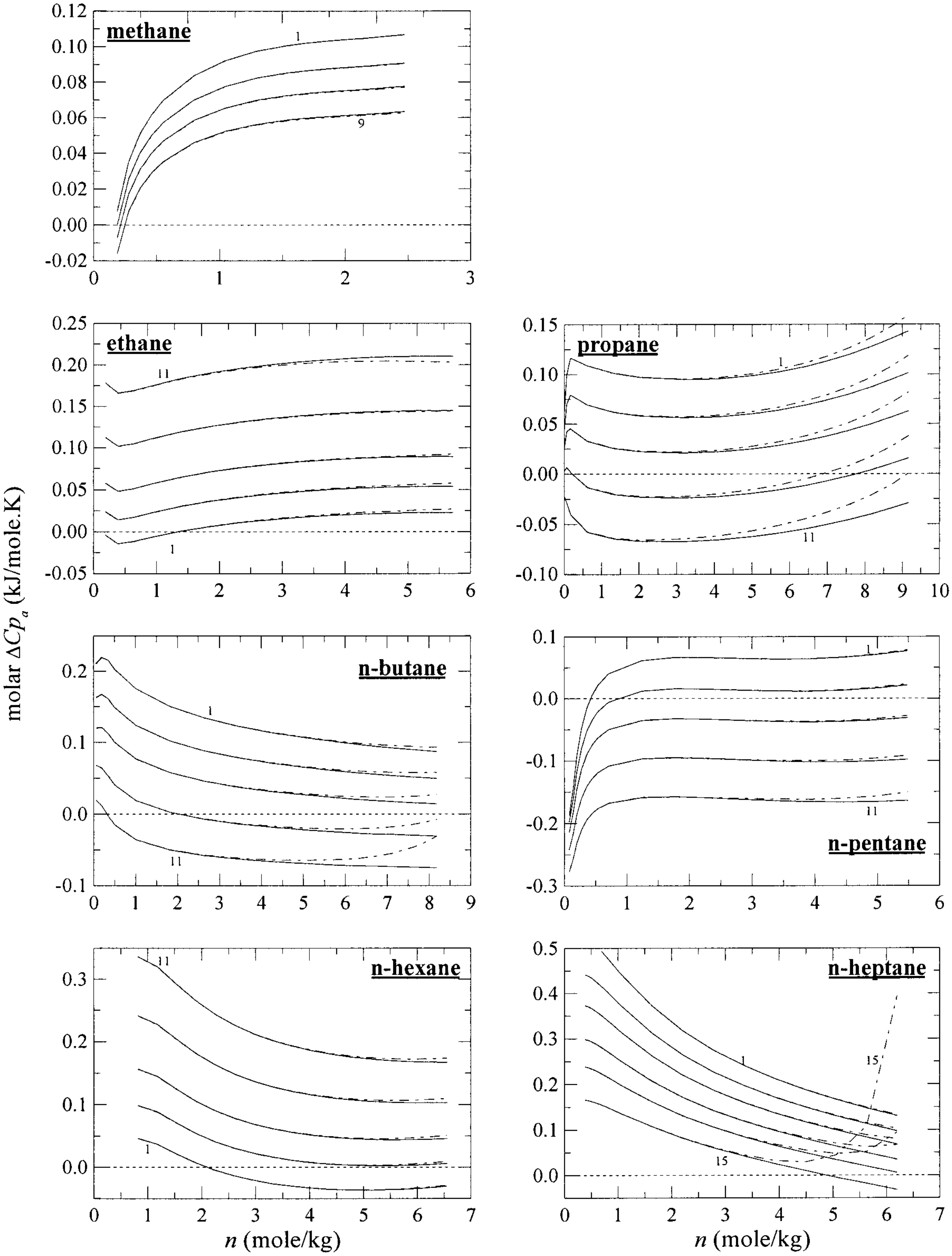

Figure 10. Comparison of real-gas (dash–dotted lines) and ideal-gas (solid lines) deviations between the molar adsorbed- and gas-phase heat capacities for the n-alkane series C_1–C_7 on BAX-1100 activated carbon predicted from the corresponding formulas derived from the SW model. Temperatures are numbered as in Figure 1.

shown in Figure 10. However, except for minor changes in the magnitudes, because of the inclusion of the spreading pressure contribution and integration, the same trends as observed in Figure 8 for the real-gas deviations between the differential adsorbed- and molar gas-phase heat capacities are observed in Figure 11 for the real-gas deviations between the molar adsorbed- and gas-phase heat capacities.

Figure 12 shows the absolute deviations between the molar adsorbed- and gas-phase heat capacities relative to the gas-phase heat capacity predicted from both the SW and VT real-gas models. Recall that the molar adsorbed-phase heat capacity is typically set equal to the molar gas-phase heat capacity in the simulation of adsorption processes. Errors as high as 200–600% resulted from this approximation for weakly adsorbed species such as methane. Adopting this approximation for more heavily adsorbed species such as hexane and heptane resulted in much lower but still serious errors ranging from 50 to 100%. The seriousness of this error

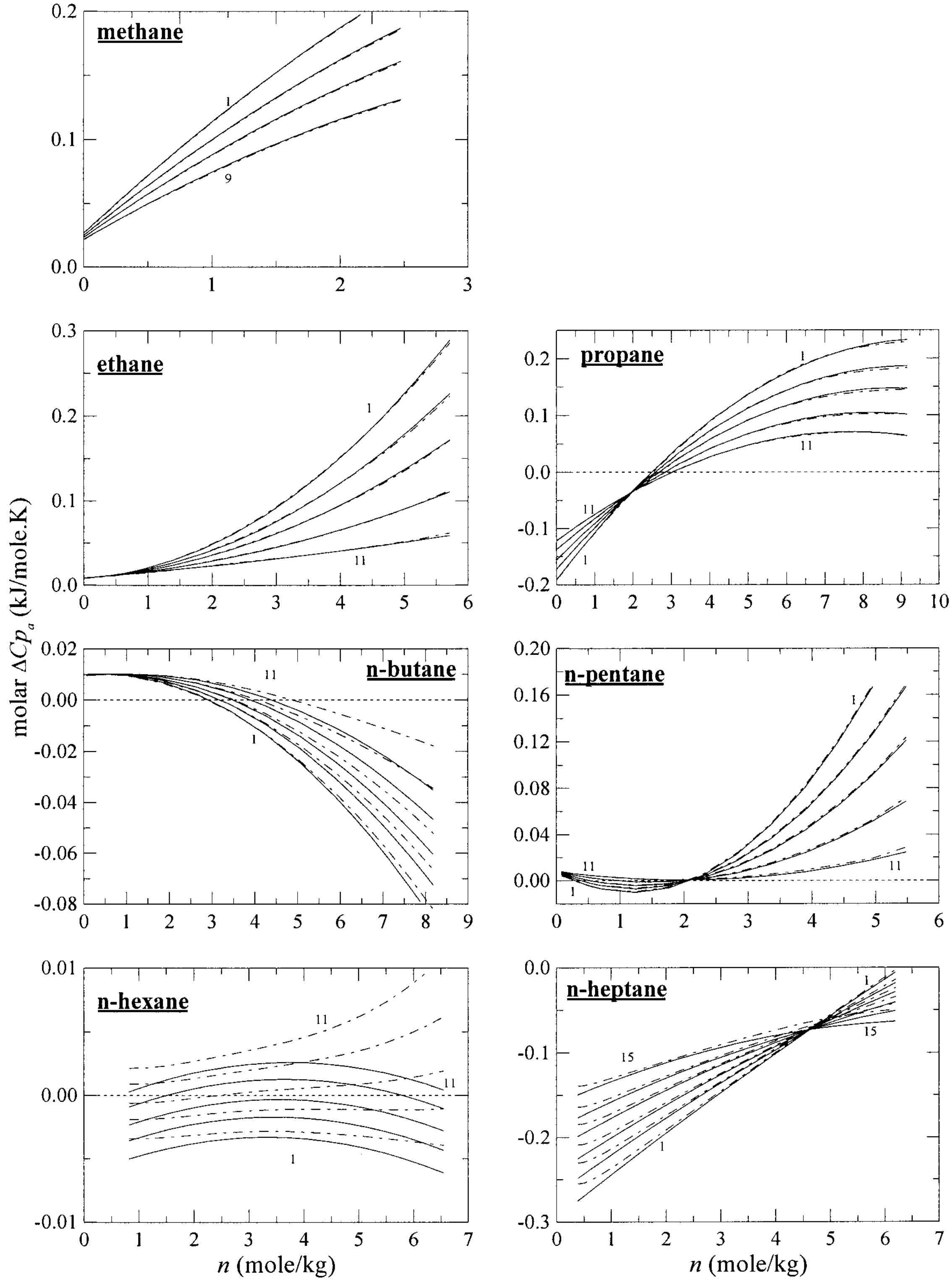

Figure 11. Comparison of real-gas (dash−dotted lines) and ideal-gas (solid lines) deviations between the molar adsorbed- and gas-phase heat capacities for the n-alkane series C_1-C_7 on BAX-1100 activated carbon predicted from the corresponding formulas derived from the VT model. Temperatures are numbered as in Figure 1.

also increased remarkably with decreasing temperature. Overall, such errors can dramatically affect the accuracy of the simulation of adsorption processes, especially those that exhibit significant heat effects.[7] Note that the VT model dramatically overestimated the errors at very high loadings of the lightly to moderately adsorbed components, for the same reasons as given earlier.

It is important to emphasize that all of the studies in the literature that discuss the temperature dependence of the isosteric heat of adsorption and the corresponding deviations between the adsorbed- and gas-phase heat capacities rely on visual verification of the linear dependence of ln(P) vs 1/T. This study shows that this first approach might result in a seeming (but possibly misleading) linear dependence between ln(P) and 1/T and that the observed linearity should be supported by evidence from the second approach explored here, i.e., a statistical analysis or fitting of the adsorption equi-

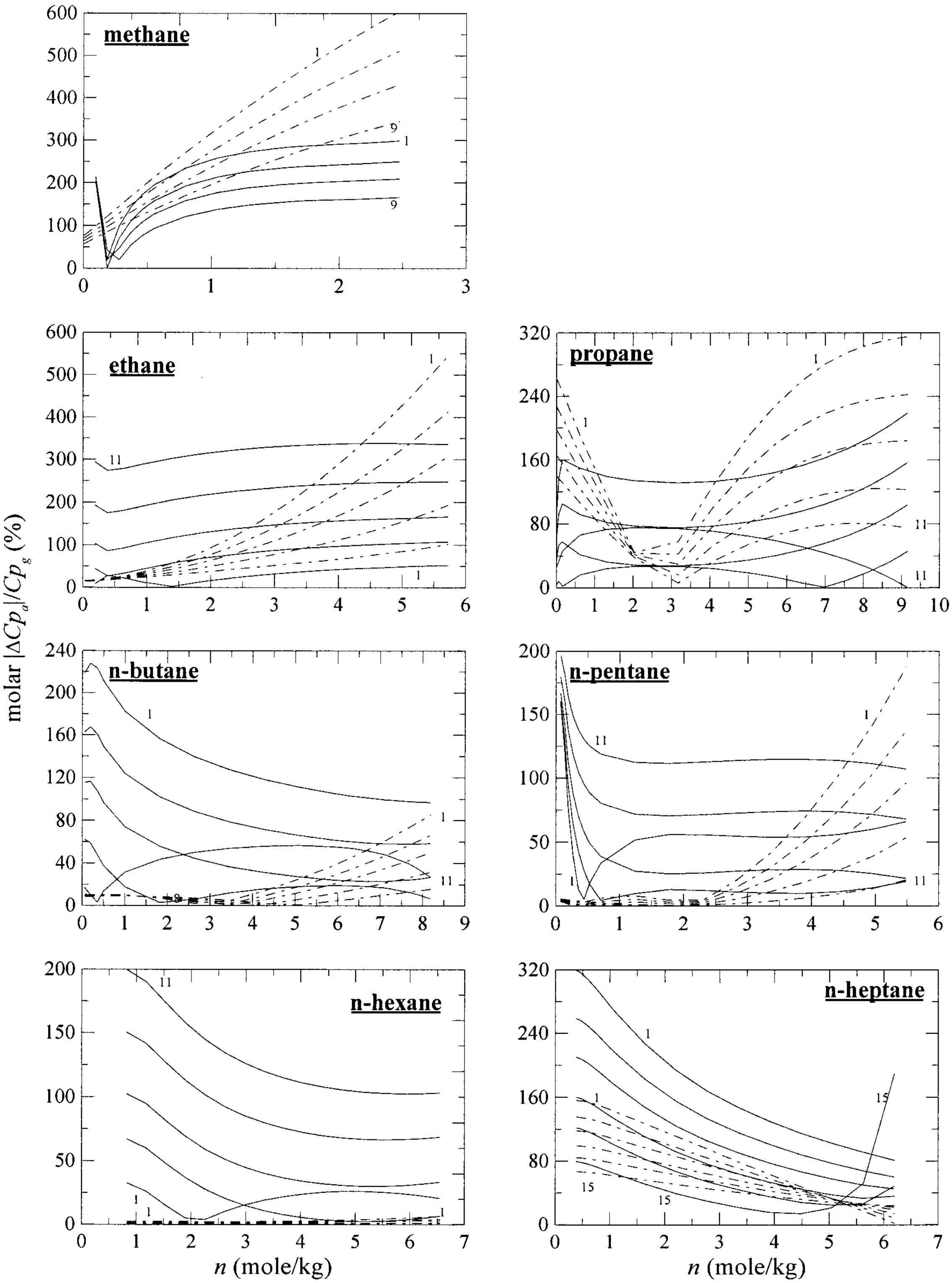

Figure 12. Absolute percent error in the deviations between the molar adsorbed- and gas-phase heat capacities relative to the gas-phase heat capacity for the n-alkane series C_1-C_7 on BAX-1100 activated carbon predicted from the real-gas formulas derived from the SW (solid lines) and VT (dash–dotted lines) models. Temperatures are numbered as in Figure 1.

libria to different pressure-explicit models.[2,8–11] This second approach reveals very weak temperature dependencies of the isosteric heat of adsorption that lead to significant deviations between the differential adsorbed- and molar gas-phase and between the molar adsorbed- and molar gas-phase heat capacities. However, direct experimental verification of the temperature dependence of the isosteric heat of adsorption and the parameters that control such a dependence is still needed.

Conclusions

The temperature dependence of the isosteric heat of adsorption can easily be overlooked when the adsorption equilibria are plotted according to the Clausius–Clapeyron equation. However, the stepwise regression model developed here was shown to be a reliable alternative for the indirect estimation of the isosteric heat of adsorption from the statistically smoothed dependence of the logarithm of the pressure on the temperature at

Table A1. Most Significant[a] Predictors from the Forward Regression of the *n*-Alkane Series C_1-C_7 Adsorption Equilibria on BAX-100 Activated Carbon[13] According to Equation 11[b]

i	*c*	*v*	*t*	*i*	*c*	*v*	*t*	*i*	*c*	*v*	*t*
	CH_4 (ARE = 11.30%)			7	−0.018266	n	−11.647	16	−7.24216E−07	n^2T^2	−1.886
1	5.649645	1	39.998	8	−9.41616E−06	$T^2 \ln n^3$	−10.227	17	−4.31502E−04	T^{-1}	−1.015
2	−0.035015	n	−10.344	9	−7.21497E−14	n^3T^{-2}	−10.070	18	1.07021E−06	nT^{-1}	0.802
3	1.82780E−07	T^3	8.106	10	9.04710E−18	n^3T^{-3}	9.937	19	−7.56210E−07	T^2n^{-1}	−0.500
4	−0.004464	$n \ln T^{-3}$	−6.430	11	2.76948E−03	T^{-1}	5.806		*n*-C_6H_{14} (ARE = 17.18%)		
5	0.002776	$T \ln n$	6.107	12	−2.75273E−12	$T^{-3} \ln n^3$	−5.479	1	6.523485	1	140.589
6	−1.82420E−05	$n^2 \ln T^2$	−6.041	13	−4.61930E−04	nT	−4.071	2	3.63860E−07	T^3	76.024
7	−0.029677	T	−5.602	14	0.027441	$\ln n^2T^{-1}$	3.829	3	−0.100649	T	−56.079
8	9.35147E−08	n^3	5.159	15	9.09368E−06	n^2	2.168	4	0.007831	$T \ln n^3$	12.961
9	6.12840E−04	nT	3.957	16	2.78639E−11	n^3T^{-1}	2.026	5	−0.034108	n	−11.289
10	−3.32207E−11	n^3T^{-2}	−3.730		*n*-C_4H_{10} (ARE = 16.98%)			6	5.07884E−05	T^2n^{-1}	9.906
11	7.55919E−11	n^2T^{-3}	3.081	1	6.216739	1	68.112	7	1.21902E−10	n^3T^{-1}	6.975
12	0.151242	$\ln n^2T^{-1}$	1.535	2	−0.069686	T	−63.131	8	7.17972E−05	n^2	6.384
13	0.025482	$\ln n^{-3}T^{-3}$	1.173	3	3.32642E−07	T^3	54.764	9	1.79057E−07	$n^{-1}T^{-3}$	5.579
	C_2H_6 (ARE = 15.85%)			4	−1.18661E−04	n^2	−17.205	10	1.52891E−05	$n^2 \ln T$	5.341
1	5.936481	1	203.064	5	0.005947	$T \ln n^3$	16.335	11	0.063674	$\ln nT$	4.749
2	−0.043337	T	−73.508	6	3.64177E−06	nT^2	14.661	12	−0.003216	$n \ln T$	−4.259
3	2.20998E−07	T^3	48.005	7	2.18201E−07	n^3	13.163	13	−1.66752E−07	n^3T	−3.594
4	−0.021870	n	−25.623	8	−3.77852E−05	$T^2 \ln n$	−12.506	14	−2.21288E−06	T^{-2}	−3.386
5	0.003911	$T \ln n^3$	21.753	9	2.18025E−06	$n^2 \ln T^3$	5.493	15	−2.79567E−06	nT^2	−2.133
6	1.86915E−6	T^{-2}	16.577	10	−5.46858E−10	$n^{-1}T^{-3}$	−2.255	16	−1.72115E−04	$n^{-1}T^{-2}$	−1.324
7	−9.02356E−12	$T^{-3} \ln n^3$	−16.208	11	0.110384	$\ln n^{-1}T^{-1}$	2.092		*n*-C_7H_{16} (ARE = 21.24%)		
8	−1.25409E−07	n^2T^{-1}	−15.022	12	3.29395E−04	$n \ln T^{-3}$	2.083	1	6.098287	1	111.988
9	−1.15525E−05	$T^2 \ln n^2$	−14.528	13	−0.026629	$\ln n^2T^{-3}$	−0.787	2	−0.078332	T	−37.574
10	2.95802E−10	n^3T^{-1}	14.375		*n*-C_5H_{12} (ARE = 15.56%)			3	2.75424E−07	T^3	22.803
11	0.042786	$\ln n^2T^{-2}$	4.759	1	6.349646	1	71.136	4	−0.018254	n	−20.935
12	2.47742E−08	n^3	4.570	2	−0.083067	T	−67.393	5	2.11137E−05	n^2	8.537
13	−1.41814E−09	n^3T^2	−3.715	3	3.82339E−07	T^3	59.005	6	4.45624E−05	nT^2	8.327
14	2.08166E−06	$n^2 \ln T^2$	3.364	4	−0.025770	n	−18.439	7	−9.83691E−07	$n^2 \ln T^{-3}$	−6.912
15	2.71746E−07	n^2T^2	2.409	5	9.40483E−08	n^3	8.702	8	3.02735E−18	n^3T^{-3}	5.304
16	4.55658E−04	nT	2.294	6	−1.04185E−08	$n^3 \ln T^{-2}$	−7.933	9	−1.97991E−14	n^3T^{-2}	−4.645
17	−1.08845E−06	nT^2	−1.375	7	2.51108E−11	T^{-3}	5.894	10	−1.51535E−07	n^3T^2	−4.473
18	−1.64099E−04	$n \ln T^{-3}$	−1.146	8	−0.001339	$n \ln T$	−4.003	11	−0.004604	nT	−4.244
	C_3H_8 (ARE = 17.02%)			9	−5.05471E−09	$n^{-1}T^{-3}$	−3.839	12	1.48908E−08	n^2T^{-1}	3.413
1	6.038566	1	120.512	10	0.004380	nT	3.640	13	−1.60281E−05	$T^2 \ln n^2$	−2.895
2	−0.057955	T	−91.351	11	−7.39045E−08	T^{-2}	−3.260	14	−1.97566E−05	T^2n^{-1}	−2.545
3	2.78470E−07	T^3	46.427	12	0.002031	$T \ln n^3$	2.713	15	−4.20640E−04	T^{-1}	−1.971
4	−6.28594E−04	$n \ln T^{-3}$	−20.540	13	0.309238	$\ln nT$	2.449	16	−0.007354	$\ln n^{-1}T^{-1}$	−0.549
5	0.006750	$T \ln n^2$	14.131	14	−0.120825	$\ln n^2T^3$	−2.154				
6	5.13845E−06	nT^2	12.255	15	−2.74433E−06	$T^2 \ln n^3$	−1.927				

[a] Largest absolute values of t that satisfied the acceptance criteria. [b] P, T and n are in atm, Kelvin, and mol/kg, respectively.

fixed loadings. This method of data smoothing has an advantage over the visual investigation of such dependencies by allowing different predictors to compete statistically in describing the objective variable. It also has an advantage over different isotherm models when considered over extremely wide pressure ranges because its formulation depends only on the specific system studied and not on any particular model formulation.

Both the stepwise (SW) regression method and the virial-type (VT) model were reasonably capable of correlating the adsorption equilibria and predicting the isosteric heats of adsorption. However, the accuracy of the temperature dependency of the isosteric heat of adsorption predicted from the virial-type model was questionable at very high amounts adsorbed, possibly indicating limitations of the use of this model over a very broad range of pressures. Both of the models agreed satisfactorily in their predictions at low-to-moderate and moderate loadings for lightly and heavily adsorbed species, respectively. The temperature-independent isosteric heat of adsorption predicted from the potential theory correlation developed in Part 1, on average, agreed reasonably well with the SW and VT model predictions for the lightly to moderately adsorbed alkanes, especially at low loadings; however, it severely underpredicted those for the heavily adsorbed alkanes.

The slight temperature dependencies of the isosteric heats of adsorption from both the SW and VT models resulted in serious deviations between the adsorbed- and gas-phase heat capacities. The seriousness of these deviations were most pronounced for low temperatures and lightly adsorbed species, with errors easily exceeding 100%. Direct experimental verification of the temperature dependence of the isosteric heat of adsorption and the corresponding deviation between the adsorbed- and gas-phase heat capacities is still needed, however.

The effect of assuming ideal-gas behavior when deriving the isosteric heat of adsorption from the Clausius−Clapeyron equation was most pronounced at high loadings and high temperatures. Correcting the isosteric heat of adsorption for real-gas conditions resulted in an overall and sometimes significant reduction in the isosteric heat of adsorption, especially at high loadings. Both the SW and the VT models behaved similarly with respect to predictions of the differences between the ideal- and real-gas isosteric heats of adsorption, but the SW model seemingly produced more reliable results.

Overall, the findings of this work are expected to be of particular importance in simulating adsorption processes over broad ranges of operating conditions and gas-phase concentrations (or adsorbed-phase loadings). Under these circumstances, it has been shown[7] that the

Table A2. Most Significant[a] Predictors from the Backward Regression of the *n*-Alkane Series C_1−C_7 Adsorption Equilibria on BAX-100 Activated Carbon[13] According to Equation 11[b]

i	*c*	*v*	*t*	*i*	*c*	*v*	*t*	*i*	*c*	*v*	*t*
	CH_4 (ARE = 8.93%)			4	−0.014941	n	−36.111	11	1.66853E−07	n^3	7.582
1	5.690267	1	66.648	5	0.004466	$T \ln n^3$	10.388	12	0.017501	$\ln n^3$	6.988
2	−0.027069	n	−22.714	6	0.001094	nT	10.360	13	4.86305E−04	n^2T	4.372
3	−0.032923	T	−15.536	7	7.15806E−04	$n \ln T^3$	9.275	14	−1.48565E−05	$T^2 \ln n$	−3.917
4	1.62447E−07	T^3	8.114	8	−4.80990E−09	nT^{-2}	−8.191	15	−1.31520E−06	n^3T	−3.906
5	1.66706E−07	$n^3 \ln T^{-1}$	8.080	9	3.22051E−18	n^3T^{-3}	7.466	16	7.22390E−12	n^3T^{-1}	3.533
6	7.63290E−08	n^3T	7.393	10	−2.66950E−05	$T^2 \ln n$	−7.306	17	1.20336E−06	n^2T^2	3.498
7	0.006833	$n \ln T^2$	7.119	11	4.23087E−03	T^{-1}	6.238		*n*-C_6H_{14} (ARE = 17.03%)		
8	−1.01932E−08	n^3T^{-1}	−4.602	12	1.70593E−08	$n^{-1}T^{-3}$	5.273	1	5.641084	1	67.289
9	−3.73267E−09	n^3T^2	−4.142	13	−1.95167E−06	$n^{-1}T^{-2}$	−5.023	2	−0.107551	T	−52.431
10	0.004337	$T \ln n^2$	3.962	14	−1.22225E−05	n^2T	−4.476	3	3.99074E−07	T^3	30.138
11	1.20080E−05	nT^2	3.803	15	5.85223E−05	$n^{-1}T^{-1}$	3.583	4	0.009891	$T \ln n^3$	14.303
12	−0.003178	nT	−3.576	16	−5.22639E−11	n^3T^{-1}	−3.125	5	−0.109129	$\ln n^3$	−10.563
13	−4.87766E−07	$T^{-3} \ln n^3$	−2.573	17	2.46232E−08	n^3T	3.107	6	6.56164E−03	T^{-1}	9.949
14	−6.42176E−06	T^{-3}	−2.570	18	1.80164E−09	$n^3 \ln T^{-3}$	2.674	7	−0.238719	$\ln n^{-1}T^{-1}$	−9.873
15	−5.88401E−06	$T^2 \ln n^3$	−2.507	19	−5.38390E−04	n^{-1}	−2.429	8	−1.62988E−03	$n^{-1}T^{-2}$	−9.036
16	0.050603	$\ln n^2T$	2.204	20	−0.008222	$\ln n^{-3}T^{-1}$	−2.100	9	−5.58443E−04	$n^{-1}T$	−8.805
17	5.97642E−02	T^{-1}	2.097	21	4.20421E−04	Tn^{-1}	2.015	10	2.16942E−03	$n^{-1}T^{-1}$	8.759
18	5.50125E−06	nT^{-2}	2.004	22	−1.15425E−06	T^2n^{-1}	−1.952	11	3.52060E−07	$n^{-1}T^{-3}$	8.385
19	6.03925E−03	$T^{-1} \ln n^2$	1.962		*n*-C_4H_{10} (ARE = 17.00%)			12	−3.70195E−04	n^2T	−6.729
20	2.94862E−13	n^3T^{-3}	1.850	1	6.174750	1	217.853	13	4.39431E−05	$n^{-1}T^2$	6.304
	C_2H_6 (ARE = 67.94%)			2	−0.071160	T	−123.399	14	8.54155E−07	n^3T	5.360
1	5.954651	1	192.768	3	3.41444E−07	T^3	65.411	15	9.46670E−07	n^2T^2	4.344
2	2.09625E−07	T^3	43.628	4	−0.019784	n	−35.933	16	−2.37786E−08	n^3	−4.092
3	−0.041911	T	−42.814	5	3.04523E−09	$n^3 \ln T^3$	17.954	17	−8.95315E−06	$T^2 \ln n^3$	−3.587
4	−0.021594	n	−23.983	6	0 0.001344	nT	15.041	18	4.08491E−04	$n \ln T^3$	3.405
5	0.006107	$T \ln n^2$	23.132	7	0 0.015771	$T \ln n$	13.705		*n*-C_7H_{16} (ARE = 21.08%)		
6	−4.57462E−18	n^3T^{-3}	−17.209	8	−3.17917E−05	$T^2 \ln n$	−9.958	1	6.343281	1	39.304
7	−1.32388E−05	$T^2 \ln n^2$	−16.538	9	3.93527E−08	n^3	8.515	2	−0.072313	T	−30.342
8	4.79287E−14	n^3T^{-2}	14.575	10	0.025382	$\ln n^2$	6.388	3	2.73033E−07	T^3	22.913
9	0.001010	$n \ln T^2$	14.299	11	−6.39868E−09	n^3T^2	−4.830	4	−6.06561E−07	n^3T^2	−10.466
10	2.51958E−06	nT^2	9.105	12	−7.10790E−07	T^{-2}	−3.450	5	−0.025951	n	−8.340
11	2.08223E−11	T^{-3}	5.255	13	1.65782E−03	T^{-1}	3.268	6	3.81263E−06	n^2T^2	7.536
12	−0.038088	$\ln n^{-3}T^{-1}$	−4.655	14	1.46546E−14	n^3T^{-2}	2.991	7	6.11661E−05	$T^2 \ln n$	6.570
13	−1.00515E−07	T^2n^{-1}	−4.241	15	1.02857E−08	$n^{-1}T^{-3}$	2.949	8	−0.006376	$T \ln n^3$	−5.175
14	−0.090487	$\ln T^2$	−3.979	16	−4.14614E−11	n^3T^{-1}	−2.693	9	3.41039E−08	$n^{-1}T^{-3}$	5.153
15	1.05837E−07	Tn^{-2}	3.522		*n*-C_5H_{12} (ARE = 15.48%)			10	9.34614E−08	n^3	4.985
16	1.63171E−08	n^3	3.399	1	6.283521	1	158.420	11	1.03153E−08	$n^3 \ln T$	4.687
17	−3.64246E−11	n^3T^{-1}	−2.937	2	−0.080537	T	−142.529	12	3.74843E−04	$n^{-1}T^{-1}$	3.763
18	−8.82278E−04	T^{-1}	−2.856	3	3.82174E−07	T^3	83.329	13	−2.03998E−04	$n^{-1}T^{-2}$	−3.882
19	−7.57111E−10	n^3T^2	−2.656	4	1.61863E−19	n^3T^{-3}	15.383	14	0.059183	$\ln n^3$	2.911
20	4.99876E−09	n^3T	2.548	5	−0.034905	n	−14.855	15	5.81281E−04	n^2T	2.837
21	−3.74324E−05	$T^{-1} \ln n^3$	−2.450	6	1.18027E−08	$n^3 \ln T^3$	8.584	16	−1.54692E−06	n^3T	−2.761
	C_3H_8 (ARE = 16.33%)			7	−7.25749E−04	T^{-1}	−8.521	17	0.104627	$\ln n^{-1}T^{-2}$	2.713
1	5.963861	1	148.253	8	0.005485	$T \ln n^2$	8.182	18	−8.90618E−05	Tn^{-1}	−2.676
2	−0.060340	T	−83.314	9	−3.29724E−07	n^3T^2	−7.957	19	7.89620E−04	T^{-1}	2.185
3	2.98755E−07	T^3	46.482	10	−0.003454	$n \ln T$	−7.852				

[a] Largest absolute values of t that satisfied the acceptance criteria. [b] P, T and n are in atm, Kelvin, and mol/kg, respectively.

temperature dependencies of the isosteric heat of adsorption and adsorbed-phase heat capacity must be accounted for if the goal is to provide more realistic process simulations. Moreover, this work exposes some of the misconceptions that result from the direct, graphical application of the Clausius−Clapeyron equation to the adsorption equilibria, and it also statistically uncovers the specific relevance of different possible forms of the temperature dependencies of the isosteric heat of adsorption and adsorbed-phase heat capacity.

Acknowledgment

The authors gratefully acknowledge financial support from the Westvaco Charleston Research Center and the Separations Research Program at the University of Texas at Austin.

Literature Cited

(1) Sircar, S.; Rao, M. B. Heat of Adsorption of Pure Gas and Multicomponent Gas Mixtures on Microporous Adsorbents. In *Surfaces of Nanoparticles and Porous Materials*; Schwarz, J. A., Contescu, C. I., Eds.; Marcel Dekker, Inc.: New York, 1999; pp 501−528.

(2) Al-Muhtaseb, S. A.; Ritter J. A. Roles of Surface Heterogeneity and Lateral Interactions on the Isosteric Heat of Adsorption and Adsorbed Phase Heat Capacity. *J. Phys. Chem. B* **1999**, *103*, 2467−2479.

(3) Dunne, J. A.; Mariwala, R.; Rao, M.; Sircar, S.; Gorte, R. J.; Myers, A. L. Calorimetric Heats of Adsorption and Adsorption Isotherms. 1. O_2, N_2, Ar, CO_2, CH_4, C_2H_6, and SF_6 on Silicate. *Langmuir* **1996**, *12*, 5888.

(4) Dunne, J. A.; Rao, M.; Sircar, S.; Gorte, R. J.; Myers, A. L. Calorimetric Heats of Adsorption and Adsorption Isotherms. 2. O_2, N_2, Ar, CO_2, CH_4, C_2H_6, and SF_6 on NaX, H−ZSM-5, and Na−ZSM-5 Zeolites. *Langmuir* **1996**, *12*, 5896.

(5) Dunne, J. A.; Rao, M.; Sircar, S.; Gorte, R. J.; Myers, A. L. Calorimetric Heats of Adsorption and Adsorption Isotherms. 3.

Mixtures of CH_4 and C_2H_6 in Salicalite and Mixtures of CO_2 and C_2H_6 in NaX. *Langmuir* **1997**, *13*, 4333.

(6) Bulow, M.; Shen, D. Sorption of Atmospheric Gases on Faujasite-type Zeolite—An Isosteric Investigation. *Fundamentals of Adsorption 6*; Meunier, F., Ed.; Elsevier: New York, 1998; pp 87−92.

(7) Liu, Y. J.; Ritter, J. A. Periodic state heat effects in pressure swing adsorption solvent vapor recovery. *Adsorption* **1998**, *4*, 159.

(8) Al-Muhtaseb, S. A.; Ritter J. A. Prediction of Single and Binary Isosteric Heats of Adsorption. *Fundamentals of Adsorption 6*; Meunier, F., Ed.; Elsevier: New York, 1998; pp 339−344.

(9) Al-Muhtaseb, S. A.; Ritter, J. A. New Virial-Type Model for Predicting Single and Multicomponent Isosteric Heats of Adsorption. *Ind. Eng. Chem. Res.* **1998**, *37*, 684−696.

(10) Al-Muhtaseb, S. A.; Ritter, J. A. Further Modification of the Antoine Equation for Correlation of Adsorption Equilibria. *Langmuir* **1998**, *14*, 5317−5323.

(11) Al-Muhtaseb, S. A.; Ritter, J. A. A Statistical Mechanic Perspective on the Temperature Dependence of the Isosteric Heat of Adsorption and Adsorbed Phase Heat Capacity. *J. Phys. Chem. B* **1999**, *103*, 8104−8115.

(12) Pan, H.; Ritter, J. A.; Balbuena, P. B. Examination of the Approximations Used in Determining the Isosteric Heats of Adsorption from the Clausius−Clapeyron Equation. *Langmuir* **1998**, *14*, 6323.

(13) Holland, C. E.; Al-Muhtaseb, S. A.; Ritter, J. A. Adsorption of C_1−C_7 Normal Alkanes on BAX Activated Carbon. 1. Measurement and Correlation of the Experimental Data. *Ind. Eng. Chem. Res.* **2001**, *40*, 338.

(14) Smith, J. M.; Van Ness, H. C. *Introduction to Chemical Engineering Thermodynamics*, 4th ed.; Mc-Graw Hill: New York, 1987; p 92.

(15) Jennrich, R. I.; Sampson, P. F. Application of stepwise regression to nonlinear estimation. *Technometrics* **1968**, *10*, 63.

(16) Jennrich, R. I. Stepwise regression. In *Statistical Methods for Digital Computers*; Enslein, K., Ralston, A., Wilf, H. S., Eds.; Wiley: New York, 1977.

(17) StatSoft, Inc. *Electronic Statistics Textbook*; StatSoft: Tulsa, OK, 1999 (http://www.statsoft.com/textbook/stathome.html, last accessed by authors in April 2000).

(18) Kapoor, A.; Ritter, J. A.; Yang, R. T. On the Dubinin−Radushkevich Equation for Adsorption in Microporous Solids in the Henry's Law Region. *Langmuir* **1989**, *5*, 1118.

(19) Ruthven, D. M. *Principles of Adsorption and Adsorption Processes*; John Wiley & Sons: New York, 1984; pp 82−84.

(20) Taqvi, S. M.; LeVan M. D. A Simple Way to Describe Nonisothermal Adsorption Equilibrium Data Using Polynomials Orthogonal to Summation. *Ind. Eng. Chem. Res.* **1997**, *36*, 419.

(21) Sundaram, N.; Yang, R. T. Isosteric heats of adsorption from gas mixtures. *J. Colloid Interface Sci.* **1998**, *198*, 378.

(22) Sircar, S. Isosteric Heats of Multicomponent Gas Adsorption on Heterogeneous Adsorbents. *Langmuir* **1991**, *7*, 3065.

Received for review May 10, 2000
Revised manuscript received September 18, 2000
Accepted September 20, 2000

IE0004803